

---

# Posterior Behavioral Cloning: Pretraining BC Policies for Efficient RL Finetuning

---

**Andrew Wagenmaker\***   **Perry Dong**   **Raymond Tsao**   **Chelsea Finn**   **Sergey Levine**  
 UC Berkeley      Stanford      UC Berkeley      Stanford      UC Berkeley

## Abstract

Standard practice across domains from robotics to language is to first pretrain a policy on a large-scale demonstration dataset, and then finetune this policy, typically with reinforcement learning (RL), in order to improve performance on deployment domains. This finetuning step has proved critical in achieving human or super-human performance, yet while much attention has been given to developing more effective finetuning algorithms, little attention has been given to ensuring the pretrained policy is an effective initialization for RL finetuning. In this work we seek to understand how the pretrained policy affects finetuning performance, and how to pretrain policies in order to ensure they are effective initializations for finetuning. We first show theoretically that standard behavioral cloning (BC)—which trains a policy to directly match the actions played by the demonstrator—can fail to ensure coverage over the demonstrator’s actions, a minimal condition necessary for effective RL finetuning. We then show that if, instead of exactly fitting the observed demonstrations, we train a policy to model the *posterior* distribution of the demonstrator’s behavior given the demonstration dataset, we *do* obtain a policy that ensures coverage over the demonstrator’s actions, enabling more effective finetuning. Furthermore, this policy—which we refer to as the *posterior behavioral cloning* (POSTBC) policy—achieves this while ensuring pretrained performance is no worse than that of the BC policy. We then show that POSTBC is practically implementable with modern generative models in robotic control domains—relying only on standard supervised learning—and leads to significantly improved RL finetuning performance on both realistic robotic control benchmarks and real-world robotic manipulation tasks, as compared to standard behavioral cloning.

## 1 Introduction

Across domains—from language, to vision, to robotics—a common paradigm has emerged for training highly effective “policies”: collect a large set of demonstrations, “pretrain” a policy via behavioral cloning (BC) to mimic these demonstrations, then “finetune” the pretrained policy on a deployment domain of interest. While pretraining can endow the policy with generally useful abilities, the finetuning step has proved critical in obtaining effective performance, enabling human value alignment and reasoning capabilities in language domains (Ouyang et al., 2022; Bai et al., 2022a; Team et al., 2025; Guo et al., 2025a), and improving task solving precision and generalization to unseen tasks in robotic domains (Nakamoto et al., 2024; Chen et al., 2025c; Kim et al., 2025; Wagenmaker et al., 2025a). In particular, reinforcement learning (RL)-based finetuning—where the pretrained policy is deployed in a setting of interest and its behavior updated based on the outcomes of these online rollouts—is especially crucial in improving the performance of a pretrained policy.

Critical to achieving successful RL-based finetuning performance in many domains—particularly in settings when policy deployment is costly and time-consuming, such as robotic control—is sample efficiency; effectively modifying the behavior of the pretrained model using as few deployment

---

\*Correspondance to: ajwagen@berkeley.edu.

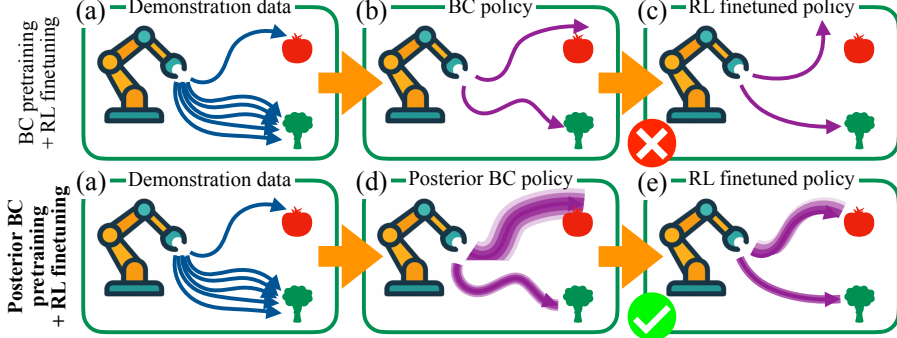


Figure 1: (a) We consider the setting where we are given demonstration data for some tasks of interest. (b) Standard BC pretraining fits the behaviors in the demonstrations, leading to effective performance in regions with high demonstration data density, yet can overcommit to the observed behaviors in regions with low data density. (c) This leads to ineffective RL finetuning, since rollouts from the BC policy provide little meaningful reward signal in such low data density regions, which is typically necessary to enable effective improvement. (d) In contrast, we propose *posterior behavioral cloning* (POSTBC), which instead of directly mimicking the demonstrations, trains a generative policy to fit the *posterior distribution* of the demonstrator’s behavior. This endows the pretrained policy with a wider distribution of actions in regions of low demonstrator data density, while in regions of high data density it reduces to approximately the standard BC policy. (e) This wider action distribution in low data density regions allows for collection of diverse observations with more informative reward signal, enabling more effective RL finetuning, while in regions of high data density performance converges to that of the demonstrator.

rollouts as possible. While significant attention has been given to developing more efficient finetuning algorithms, this ignores a primary ingredient in the RL finetuning process: the pretrained policy itself. Though generally more effective pretrained policies are the preferred initialization for finetuning (Guo et al., 2025a; Yue et al., 2025), it is not well understood how pretraining impacts finetuning performance beyond this, and how we might pretrain policies to enable more efficient RL finetuning.

In this work we seek to understand the role of the pretrained policy in RL finetuning, and how we might pretrain policies that (a) enable efficient RL finetuning, and (b) before finetuning, perform no worse than the policy pretrained with standard BC. We propose a novel pretraining approach—*posterior behavioral cloning* (POSTBC)—which, rather than fitting the empirical distribution of demonstrations as standard BC does, instead fits the *posterior* distribution over the demonstrator’s behavior. That is, assuming a uniform prior over the demonstrator’s behavior and viewing the demonstration data as samples from the demonstrator’s behavioral distribution, we seek to train a policy that models the posterior distribution of the demonstrator’s behavior given these observations. This enables the pretrained policy to take into account its potential uncertainty about the demonstrator’s behavior, and adjust the entropy of its action distribution based on this uncertainty. In states where it is uncertain about the demonstrator’s actions, POSTBC samples from a high-entropy distribution, allowing for a more diverse set of actions that may enable further policy improvement, while in states where it is certain about the demonstrator’s actions, it samples from a low-entropy distribution, simply mimicking what it knows to be the (correct) demonstrator behavior (see Figure 1).

Theoretically, we show that POSTBC leads to provable improvements over standard BC in terms of the potential for downstream RL performance. In particular, we focus on the ability of the pretrained policy to cover the demonstrator policy’s actions—whether it samples all actions the demonstrator policy might sample—which, for finetuning approaches that rely on rolling out the pretrained policy, is a prerequisite to ensure finetuning can even match the performance of the demonstrator. We show that standard BC can provably fail to cover the demonstrator’s distribution, while POSTBC *does* cover the demonstrator’s distribution, incurs no suboptimality in the performance of the pretrained policy as compared to the standard BC policy, and achieves a near-optimal sampling cost out of all policy estimators which have pretrained performance no worse than the BC policy’s.

Inspired by this, we develop a practical approach to approximating the posterior of the demonstrator in continuous action domains, and instantiate POSTBC with modern generative models—diffusion models—on robotic control tasks. Our instantiation relies only on pretraining with scalable supervised learning objectives—no RL is required in pretraining—and can be incorporated into existing

BC training pipelines with minimal modification. We demonstrate experimentally that POSTBC pretraining can lead to significant performance gains in terms of the efficiency and effectiveness of RL finetuning, as compared to running RL finetuning on a policy pretrained with standard BC, and achieves these gains without decreasing the performance of the pretrained policy itself. We show that this holds for a variety of finetuning algorithms—both policy-gradient-style algorithms, and algorithms which explicitly refine or filter the distribution of the pretrained policy—enabling effective RL finetuning across a variety of challenging robotic tasks in both simulation and the real world.

## 2 Related Work

**BC pretraining.** BC training of expressive generative models—where the model is trained to predict the next “action” of the demonstrator—forms the backbone of pretraining for LLMs (Radford et al., 2018) and robotic control (Bojarski, 2016; Zhang et al., 2018; Rahmatizadeh et al., 2018; Stepputtis et al., 2020; Shafiuallah et al., 2022; Gu et al., 2023; Team et al., 2024; Zhao et al., 2024; Black et al., 2024; Kim et al., 2024). Experimentally, we focus in particular on policies parameterized as diffusion models (Sohl-Dickstein et al., 2015; Ho et al., 2020; Song et al., 2020), which have seen much attention in the robotics community (Chi et al., 2023; Ankile et al., 2024a; Zhao et al., 2024; Ze et al., 2024; Sridhar et al., 2024; Dasari et al., 2024; Team et al., 2024; Black et al., 2024; Bjorck et al., 2025), yet our approach can extend to other generative model classes as well. These works, however, simply pretrain with standard BC, and do not consider how the pretraining may affect RL finetuning performance. Please see Section A for a discussion of other approaches to pretraining (imitation learning, meta-learning, and reinforcement learning).

**Pretraining for downstream finetuning.** Several recent works in the language domain aim to understand the relationship between pretraining and downstream finetuning (Springer et al., 2025; Zeng et al., 2025; Chen et al., 2025b; Jin et al., 2025; Chen et al., 2025a). A common thread through these works is that cross entropy loss is not predictive of downstream finetuning performance, and, in fact, low cross entropy loss can be anti-correlated with finetuning performance as the model can become *overconfident*. Most related to our work is the concurrent work of Chen et al. (2025a), which consider a notion of *coverage* closely related to our notion of *demonstrator action coverage*, and show that coverage generalizes faster than cross-entropy, and is an effective predictor of the downstream success of Best-of- $N$  sampling. While both our work and Chen et al. (2025a) focus on notions of coverage to enable downstream improvement, we see this work as complementary. While Chen et al. (2025a) show coverage generalizes faster than cross-entropy, our results show BC pretraining can *still* fail to ensure meaningful coverage, especially in the small sample regime. Furthermore, Chen et al. (2025a) does not consider the tradeoff between policy performance and coverage that is a primary focus of our work, and their proposed pretraining intervention—gradient normalization—would not resolve the shortcomings of BC in our setting, while our proposed intervention, POSTBC, does. Finally, Chen et al. (2025a) is primarily a theoretical work and focuses on discrete next-token prediction (indeed, all works cited above consider only discrete next-token prediction); in contrast, a primary focus of our work is on continuous control, and we demonstrate our approach scales to real-world robotic settings.

**RL finetuning of pretrained policies.** RL finetuning of pretrained policies is a critical step in both language and robotic domains. In language domains, RL finetuning has proved crucial in aligning LLMs to human values (Ziegler et al., 2019; Ouyang et al., 2022; Bai et al., 2022a; Ramamurthy et al., 2022; Touvron et al., 2023), and enabling reasoning abilities (Shao et al., 2024; Team et al., 2025; Guo et al., 2025a). A host of finetuning algorithms have been developed, both online (Bai et al., 2022b; Bakker et al., 2022; Dumoulin et al., 2023; Lee et al., 2023; Munos et al., 2023; Swamy et al., 2024; Chakraborty et al., 2024; Chang et al., 2024) and offline (Rafailov et al., 2023; Azar et al., 2024; Rosset et al., 2024; Tang et al., 2024; Yin et al., 2024). In robotic control domains, RL finetuning methods include directly modifying the weights of the base pretrained policy (Zhang et al., 2024; Xu et al., 2024; Mark et al., 2024; Ren et al., 2024; Hu et al., 2025; Guo et al., 2025b; Lu et al., 2025; Chen et al., 2025c; Liu et al., 2025), Best-of- $N$  sampling-style approaches that filter the output of the pretrained policy with a learned value function (Chen et al., 2022; Hansen-Estruch et al., 2023; He et al., 2024; Nakamoto et al., 2024; Dong et al., 2025b), “steering” the pretrained policy by altering its sampling process (Wagenmaker et al., 2025a), and learning smaller residual policies to augment the pretrained policy’s actions (Ankile et al., 2024b; Yuan et al., 2024; Jülg et al., 2025; Dong et al., 2025a). Our work is tangential to this line of work: rather than improving the finetuning algorithm, we aim to ensure the pretrained policy is amenable to RL finetuning.

**Posterior sampling and exploration.** Our proposed approach relies on modeling the posterior distribution of the demonstrator’s behavior. While this is, to the best of our knowledge, the first example of applying posterior sampling to BC, posterior methods have a long history in RL, going back to the work of Thompson (1933). This works spans applied (Osband et al., 2016a,b, 2018; Zintgraf et al., 2019) and theoretical (Agrawal & Goyal, 2012; Russo & Van Roy, 2014; Russo et al., 2018; Janz et al., 2024; Kveton et al., 2020; Russo, 2019) settings. More generally, our approach can be seen as enabling BC-trained policies to *explore* more effectively. Exploration is a well-studied problem in the RL community (Stadie et al., 2015; Bellemare et al., 2016; Burda et al., 2018; Choi et al., 2018; Ecoffet et al., 2019; Shyam et al., 2019; Lee et al., 2021; Henaff et al., 2022), with several works considering learning exploration strategies from offline data (Hu et al., 2023; Li et al., 2023a; Wilcoxson et al., 2024; Wagenmaker et al., 2025b). These works, however, either consider RL-based pretraining (while we focus on BC) or do not consider the question of online finetuning.

### 3 Preliminaries

**Mathematical notation.** Let  $\lesssim$  denote inequality up to absolute constants,  $\Delta_{\mathcal{X}}$  the simplex over  $\mathcal{X}$ , and  $\text{unif}(\mathcal{X})$  the uniform distribution over  $\mathcal{X}$ .  $\mathbb{I}\{\cdot\}$  denotes the indicator function,  $\mathbb{E}^{\pi}[\cdot]$  the expectation under policy  $\pi$  and, unless otherwise noted,  $\mathbb{E}[\cdot]$  the expectation over the demonstrator dataset.

**Markov decision processes.** We consider decision-making in the context of episodic, fixed-horizon Markov decision processes (MDPs). An MDP  $\mathcal{M}$  is denoted by a tuple  $(\mathcal{S}, \mathcal{A}, \{P_h\}_{h=1}^H, P_0, r, H)$ , where  $\mathcal{S}$  is the set of states,  $\mathcal{A}$  the set of actions,  $P_h : \mathcal{S} \times \mathcal{A} \rightarrow \Delta_{\mathcal{S}}$  the next-state distribution at step  $h$ ,  $P_0 \in \Delta_{\mathcal{S}}$  the initial state distribution,  $r_h : \mathcal{S} \times \mathcal{A} \rightarrow \Delta_{[0,1]}$  the reward distribution, and  $H$  the horizon. Interaction with  $\mathcal{M}$  proceeds in episodes of length  $H$ . At step 1, we sample a state  $s_1 \sim P_0$ , take an action  $a_1 \in \mathcal{A}$ , receive reward  $r_1(s_1, a_1)$ , and transition to state  $s_2 \sim P_1(\cdot | s_1, a_1)$ . This continues for  $H$  steps until the MDP resets. We let  $\mathcal{J}(\pi) := \mathbb{E}^{\pi}[\sum_{h=1}^H r_h(s_h, a_h)]$  denote the expected reward for policy  $\pi$ . In general, our goal is to find a policy that maximizes  $\mathcal{J}(\pi)$ .

**Behavioral cloning.** We assume we are given some dataset  $\mathfrak{D} = \{(s_1^t, a_1^t, \dots, s_H^t, a_H^t)\}_{t=1}^T$  collected by running a *demonstrator* policy  $\pi^{\beta}$  on  $\mathcal{M}$ , so that  $(s_1^t, a_1^t, \dots, s_H^t, a_H^t)$  denotes a trajectory rollout of  $\pi^{\beta}$  on  $\mathcal{M}$ , with  $a_h^t \sim \pi_h^{\beta}(\cdot | s_h^t)$ . We assume that  $\pi^{\beta}$  is Markovian but otherwise make no further assumptions on it (so, in particular,  $\pi^{\beta}$  may be stochastic and suboptimal). Our demonstrator dataset does not include reward labels—preventing standard offline RL approaches from applying—but we assume that we have access to reward labels during online interactions.

*Behavioral cloning* (BC) attempts to fit a policy  $\hat{\pi}^{\text{bc}}$  to match the distribution of actions observed in  $\mathfrak{D}$ . Typically this is achieved via supervised learning, where  $\hat{\pi}^{\text{bc}}$  is trained to predict  $a$  given  $s$  for  $(s, a) \in \mathfrak{D}$ . In the tabular setting, which we consider in Section 4, the natural choice for  $\hat{\pi}^{\text{bc}}$  models the empirical action distribution in  $\mathfrak{D}$ :

$$\hat{\pi}_h^{\text{bc}}(a | s) := \begin{cases} \frac{T_h(s, a)}{T_h(s)} & T_h(s) > 0 \\ \text{unif}(\mathcal{A}) & T_h(s) = 0, \end{cases} \quad (1)$$

where  $T_h(s, a) = \sum_{t=1}^T \mathbb{I}\{(s_h^t, a_h^t) = (s, a)\}$  and  $T_h(s) = \sum_{t=1}^T \mathbb{I}\{s_h^t = s\}$ . The following result bounds the suboptimality of this estimator, and shows that it is optimal, up to log factors.

**Proposition 1** (Rajaraman et al. (2020)). *If  $\mathfrak{D}$  contains  $T$  demonstrator trajectories, we have*

$$\mathcal{J}(\pi^{\beta}) - \mathbb{E}[\mathcal{J}(\hat{\pi}^{\text{bc}})] \lesssim \frac{H^2 S \log T}{T}.$$

*Furthermore, for any estimator  $\hat{\pi}$ , there exists some MDP  $\mathcal{M}$  and demonstrator  $\pi^{\beta}$  such that*

$$\mathcal{J}(\pi^{\beta}) - \mathbb{E}[\mathcal{J}(\hat{\pi})] \gtrsim \min \left\{ H, \frac{H^2 S}{T} \right\}.$$

In other words, without additional reward information, we cannot in general hope to obtain a policy from  $\mathfrak{D}$  that does better than (1), if our goal is to maximize the performance of the pretrained policy. Note that the BC estimator in (1) is, under the uniform demonstrator prior (i.e. the prior under which the demonstrator is equally likely to play each action in each state), the *maximum a posterior* (MAP) estimate of the demonstrator’s behavior.

## 4 Achieving Demonstrator Action Coverage via Posterior Sampling

In this section we seek to understand how pretraining affects the ability to further improve the downstream policy with RL finetuning, and how we might pretrain to enable downstream improvement. For simplicity, here we assume that our MDP  $\mathcal{M}$  is tabular, and let  $S$  and  $A$  denote the cardinalities of the state and action spaces, respectively; we will show how our proposed approach can be extended to more general settings in the following section.

### 4.1 Demonstrator Action Coverage

The performance of RL finetuning depends significantly on the RL algorithm applied. Rather than limiting our results to a particular RL algorithm, we instead focus on what is often a prerequisite for effective application of any such approach—demonstrating that the *support* of the pretrained policy is sufficient to enable improvement. In particular, we consider the following definition for the “effective” support of a policy, relative to the demonstrator policy  $\pi^\beta$ .

**Definition 4.1** (Demonstrator Action Coverage). We say policy  $\pi$  achieves demonstrator action coverage with parameter  $\gamma > 0$  if, for all  $(s, h) \in \mathcal{S} \times [H]$  and  $a \in \mathcal{A}$ , we have  $\pi_h(a | s) \geq \gamma \cdot \pi_h^\beta(a | s)$ .

The majority of RL finetuning approaches rely on rolling out the pretrained policy—which we denote as  $\hat{\pi}^{\text{pt}}$ —online, and using the collected observations to finetune its behavior. If our pretrained policy achieves demonstrator action coverage with parameter  $\gamma$ , then this ensures that any action sampled by  $\pi^\beta$  will also be sampled by  $\hat{\pi}^{\text{pt}}$  in these rollouts (with some probability). While this is not a *sufficient* condition for online improvement, it is a *necessary* condition, in some cases, for performing as well as the demonstrator  $\pi^\beta$  (as Proposition 2 in the following shows), and is therefore also a necessary condition for improving over  $\pi^\beta$ . Furthermore, the *value* of  $\gamma$  has impact on the cost of RL finetuning. A policy  $\pi$  which achieves demonstrator action coverage with parameter  $\gamma$  requires a factor of  $1/\gamma$  more samples than  $\pi^\beta$  to ensure it samples some action in the support of  $\pi^\beta$ . For approaches such as Best-of- $\bar{N}$  sampling that rely on sampling many actions from the pretrained policy and then taking the best one, a large value of  $\gamma$  therefore ensures we can efficiently sample actions likely to be sampled by the demonstrator policy  $\pi^\beta$ , while if  $\gamma$  is small, it may take a significant number of samples to sample an action necessary for improvement. In addition, a small value of  $\gamma$  may impact the statistical cost of RL finetuning—for small  $\gamma$  we may require a large number of online rollouts to observe the behavior of actions that  $\pi^\beta$  plays, which is necessary to ensure we can match the performance of  $\pi^\beta$  after RL finetuning.

**Problem Statement: Demonstrator Action Coverage with BC-Pretrained Performance.** In the following, we aim to understand how we can pretrain policies that achieve demonstrator action coverage with values of  $\gamma$  as large as possible. Furthermore, we aim to achieve this without incurring significant additional suboptimality as compared to  $\hat{\pi}^{\text{bc}}$ , the BC-pretrained policy—we would like to ensure that  $\hat{\pi}^{\text{pt}}$  is an effective initialization for finetuning while still itself achieving performance comparable to the BC policy, the optimal policy judged on pretrained performance alone.

### 4.2 Behavioral Cloning Fails to Achieve Demonstrator Action Coverage

We first consider standard BC, i.e. (1). The following result shows that the estimator in (1), despite achieving the best possible suboptimality rate, can fail to achieve a meaningful guarantee on demonstrator action coverage, and that this fundamentally limits its ability to serve as an effective initialization for finetuning.

**Proposition 2.** Fix  $\epsilon \in (0, 1/8]$ . Then there exist some MDPs  $\mathcal{M}^1, \mathcal{M}^2$  and demonstrator policy  $\pi^\beta$  such that, if  $\mathcal{M} \in \{\mathcal{M}^1, \mathcal{M}^2\}$ , unless  $T \geq \frac{1}{20\epsilon}$ , we have that, with probability at least  $1/2$ :

$$\mathcal{J}(\pi^\beta) - \epsilon > \max_{\pi \in \hat{\Pi}} \mathcal{J}(\pi) \quad \text{for} \quad \hat{\Pi} := \{\pi : \pi_h(a | s) = 0 \text{ if } \hat{\pi}_h^{\text{bc}}(a | s) = 0, \forall s, a, h\}.$$

Furthermore, for any  $T' > 0$ ,

$$\min_{\hat{\pi}^{T'}} \max_{i \in \{1, 2\}} \mathbb{E}^{\mathcal{M}^i, \hat{\pi}^{\text{bc}}} [\max_{\pi} \mathcal{J}^{\mathcal{M}^i}(\pi) - \mathcal{J}^{\mathcal{M}^i}(\hat{\pi}^{T'})] \geq \frac{1}{2},$$

where  $\mathbb{E}^{\mathcal{M}^i, \hat{\pi}^{\text{bc}}}[\cdot]$  denotes the expectation over trajectories generated by rolling out  $\hat{\pi}^{\text{bc}}$  on  $\mathcal{M}^i$ , and  $\hat{\pi}^{T'}$  is a policy estimator obtained after  $T'$  such rollouts.

Proposition 2 shows that, unless we have a sufficiently large demonstration dataset, half of the time (i.e. half of the random draws of the demonstrator dataset) the policy returned by standard BC will not contain a near-optimal policy in its support and, furthermore, that rolling out  $\hat{\pi}^{\text{bc}}$  on  $\mathcal{M}$  will not allow us to learn a near-optimal policy on  $\mathcal{M}$ . In other words, some fraction of the time standard BC produces a policy which cannot be improved with RL finetuning approaches that rely on rolling out the pretrained policy. Furthermore, this shows that demonstrator action coverage is, in some cases, a necessary condition for successful RL improvement—without this, we simply will not sample actions played by the demonstrator, and will therefore be unable to determine which actions actually lead to the best performance.

The key failing of BC in Proposition 2 is that, if it has not yet observed the demonstrator play an action, it will simply not play this action—it overfits to the actions it has observed. A straightforward solution to this is to simply add exploration noise to our pretrained policy—rather than playing  $\hat{\pi}^{\text{bc}}$  at every step, with some probability play a random action. While this will clearly address the shortcoming of BC outlined above—the pretrained policy will now play *every* action—as the following result shows, there is a fundamental tradeoff between the suboptimality of this policy and the number of samples from the policy required to achieve demonstrator action coverage.

**Proposition 3.** *Fix  $T > 0$ ,  $H \geq 2$ ,  $S \geq \lceil \log_2 4T \rceil + 2$ ,  $\xi \geq 0$ , define  $\epsilon := \frac{H^2 S \log T}{T} + \xi$ , and assume  $\epsilon \leq \frac{1}{2}$ . Define the policy  $\hat{\pi}^{\text{u},\alpha}$  as  $\hat{\pi}_h^{\text{u},\alpha}(\cdot | s) := (1 - \alpha) \cdot \hat{\pi}_h^{\text{bc}}(\cdot | s) + \alpha \cdot \text{unif}(\mathcal{A})$ . Then there exists some MDP  $\mathcal{M}$  with  $S$  states, 2 actions, and horizon  $H$  where, in order to ensure that:*

1.  $\mathcal{J}(\pi^\beta) - \mathbb{E}[\mathcal{J}(\hat{\pi}^{\text{u},\alpha})] \leq \epsilon$ ,
2.  $\hat{\pi}^{\text{u},\alpha}$  achieves demonstrator action coverage with parameter  $\gamma$  and probability at least  $1 - \delta$ , for  $\delta \in (0, 1/4e)$ ,

we must have  $\alpha \leq 32\epsilon$  and  $\gamma \leq \frac{64}{A} \cdot \epsilon$ . Furthermore, with probability at least  $1/4e$ , we have

$$\mathcal{J}(\pi^\beta) - \frac{1}{T} \cdot \epsilon > \max_{\pi \in \hat{\Pi}} \mathcal{J}(\pi) \quad \text{for } \hat{\Pi} := \{\pi : \pi_h(a | s) = 0 \text{ if } \hat{\pi}_h^{\text{bc}}(a | s) = 0, \forall s, a, h\}.$$

In order to achieve the  $\frac{H^2 S \log T}{T}$  suboptimality rate achieved by standard BC, Proposition 3 then shows that we can only guarantee demonstrator action coverage with parameter  $\gamma \lesssim \frac{1}{A} \cdot \frac{H^2 S \log T}{T}$ . Or, in other words, to ensure we sample a particular action from  $\hat{\pi}^{\text{u},\alpha}$  that is sampled by  $\pi^\beta$ , it will require sampling a factor of  $\frac{AT}{H^2 S \log T}$  more samples from  $\hat{\pi}^{\text{u},\alpha}$  than it would require from  $\pi^\beta$ . While this does enable RL improvement from rolling out the pretrained policy, in settings where  $T$  is large it could require a significant number of samples from the pretrained policy to achieve this, greatly increasing the cost of such an approach. Furthermore, Proposition 3 shows that this limitation is critical—if we seek to shortcut this exploration and set  $\alpha \leftarrow 0$ , we will fail to match the performance of  $\pi^\beta$  on this instance completely.

### 4.3 Posterior Demonstrator Policy Achieves Demonstrator Action Coverage

Can we do better than BC or BC augmented with uniform noise? Here we show that a mixture of the standard BC policy and the *posterior* on the demonstrator’s policy achieves a near optimal balance between policy suboptimality and demonstrator action coverage.

**Definition 4.2** (Posterior Demonstrator Policy). Given prior distribution  $P_{\text{prior}}^\beta \in \Delta_\Pi$  over demonstrator policies, let  $P_{\text{post}}^\beta(\cdot | \mathcal{D})$  denote the posterior distribution given demonstration dataset  $\mathcal{D}$ . We then define the *posterior demonstrator policy*  $\hat{\pi}^{\text{post}}$  as  $\hat{\pi}_h^{\text{post}}(a | s) := \mathbb{E}_{\pi \sim P_{\text{post}}^\beta(\cdot | \mathcal{D})} [\pi_h(a | s)]$ .

$\hat{\pi}^{\text{post}}$  is therefore the expected posterior policy of the demonstrator under prior  $P_{\text{prior}}^\beta$  given observations  $\mathcal{D}$ . Critically, this takes into account the entire posterior distribution of the demonstrator’s behavior, in contrast to the MAP estimate produced by standard BC, which simply returns a point estimate of the behavior. In the tabular setting, some algebra shows that

$$\hat{\pi}_h^{\text{post}}(a | s) = \begin{cases} \frac{T_h(s, a) + 1}{T_h(s) + A} & T_h(s) > 0 \\ \text{unif}(\mathcal{A}) & T_h(s) = 0, \end{cases}$$

so that  $\hat{\pi}_h^{\text{post}}(a \mid s)$  increases the weight on actions for which  $T_h(s, a)$  is very small, as compared to the BC policy. In practice, we require a slightly regularized version of  $\hat{\pi}^{\text{post}}$ ,  $\hat{\pi}^{\text{post}, \lambda}$ , which is identical to  $\hat{\pi}^{\text{post}}$  if  $HT \lesssim e^A$ , and otherwise adds a small amount of additional regularization (see Section B.3 for a precise definition). We have the following.

**Theorem 1.** *Let  $P_{\text{prior}}^\beta$  be the uniform distribution over Markovian policies, and set  $\hat{\pi}^{\text{pt}}$  to*

$$\hat{\pi}_h^{\text{pt}}(a \mid s) = (1 - \alpha) \cdot \hat{\pi}_h^{\text{bc}}(a \mid s) + \alpha \cdot \hat{\pi}_h^{\text{post}, \lambda}(a \mid s) \quad (2)$$

for  $\alpha = \frac{1}{\max\{A, H, \log(HT)\}}$ . Then

$$\mathcal{J}(\pi^\beta) - \mathbb{E}[\mathcal{J}(\hat{\pi}^{\text{pt}})] \lesssim \frac{H^2 S \log T}{T},$$

and with probability at least  $1 - \delta$ , for all  $(s, a, h)$ ,

$$\hat{\pi}_h^{\text{pt}}(a \mid s) \gtrsim \frac{1}{A + H + \log(HT)} \cdot \min \left\{ \frac{\pi_h^\beta(a \mid s)}{\log(SH/\delta)}, \frac{1}{A + \log(HT)} \right\}.$$

Theorem 1 shows that by setting  $\hat{\pi}^{\text{pt}}$  to a mixture of the BC policy and the posterior demonstrator policy, we obtain the same suboptimality guarantee as standard BC. Furthermore, this policy achieves demonstrator action coverage with  $\gamma \approx 1/(A + H)$ , only requiring a factor of  $\approx A + H$  more samples to ensure we sample a particular action from  $\pi^\beta$  than  $\pi^\beta$  itself does (for actions  $a$  such that  $\pi_h^\beta(a \mid s) \lesssim 1/A$ , and otherwise requires at most a factor of  $A(A + H)$  more). We refer to this approach as *posterior behavioral cloning* (POSTBC). The following result shows that the scaling in  $\gamma$  POSTBC achieves is nearly unimprovable.

**Theorem 2.** *Fix any  $A > 1$  and  $T > 1$ . Then there exists a family of MDPs  $\{\mathcal{M}^i\}_{i \in [A]}$  such that each  $\mathcal{M}^i$  has  $A$  actions and  $S = H = 1$ , and if any estimator  $\hat{\pi}$  satisfies  $\mathcal{J}^{\mathcal{M}^i}(\pi^{\beta, i}) - \mathbb{E}^{\mathcal{M}^i}[\mathcal{J}(\hat{\pi})] \leq c \cdot \frac{H^2 S \log T}{T}$  for all  $i \in [A]$  and some constant  $c > 0$ , then for  $\hat{\pi}$  to achieve demonstrator action coverage with respect to  $\pi^{\beta, i}$  on each  $\mathcal{M}^i$  with probability at least  $\delta \in (0, 1/4]$ , we must have  $\gamma \leq c \cdot \frac{\log T}{A}$ .*

Theorem 2 shows that, to match the suboptimality guarantee of the BC policy, no estimator can achieve demonstrator action coverage with  $\gamma$  larger than  $\approx 1/A$ . Thus, the demonstrator action coverage achieved by POSTBC is nearly unimprovable, matching the lower bound as long as  $H \leq A$ . In other words, if we want a policy that preserves the optimality of  $\hat{\pi}^{\text{bc}}$  while playing a diverse enough action distribution to enable further online improvement, mixing the posterior demonstrator policy with the BC policy achieves a near-optimal tradeoff, playing all actions taken by  $\pi^\beta$  with minimal additional sampling and matching the pretrained performance of the BC policy. This is in contrast to the BC policy, which does not achieve a meaningful guarantee on demonstrator action coverage, as well as the BC policy augmented with random exploration, which in order to match the suboptimality of the BC policy achieves a very suboptimal guarantee on demonstrator action coverage.

The key insight behind the performance of POSTBC is that, if we add entropy to the action distribution at each state proportional to our uncertainty about the demonstrator’s behavior at that state, this will not hurt the performance relative to the BC policy. Intuitively, if we are not certain what the demonstrator’s behavior is at a given state, the BC policy may or may not be correct at this state, so adding additional entropy will not make it worse—we are simply selecting the maximum entropy distribution that *might* explain the observations produced by the demonstrator. POSTBC expands the action distribution enough to ensure that we cover the demonstrator’s true action distribution at such states, while at states where we have enough observations to accurately estimate the demonstrator’s action distribution, POSTBC will decrease entropy to simply match this distribution. This is in contrast to the behavior induced by uniformly adding entropy as in Proposition 3—while we want to add significant entropy to states where we are uncertain about the demonstrator’s behavior, if we add this entropy to states where we *are* certain the performance could drop significantly below that of the demonstrator, greatly limiting the amount of entropy we can add uniformly.

## 5 Practical Posterior Behavioral Cloning

The previous section suggests a simple recipe to obtain a pretrained policy amenable to online improvement: compute the posterior demonstrator policy given the demonstration data, then mix the posterior demonstrator policy with the BC-pretrained policy. In this section we show how this can be instantiated in continuous control settings using expressive generative policy classes. To this end, in Section 5.1 we first consider a simplified Gaussian setting, and in Section 5.2 seek to generalize the insights from this simplified setting to more complex domains.

## 5.1 Sampling from the Posterior Demonstrator Policy for Gaussian Demonstrators

To motivate our practical instantiation, consider the setting where:

$$\pi_h^\beta(\cdot | s) = \mathcal{N}(\mu_h(s), \sigma_h^2(s) \cdot I),$$

for some (unknown)  $\mu_h(s) \in \mathbb{R}^d$  and (known)  $\sigma_h(s) \in \mathbb{R}$ . Assume we have observations  $\mathfrak{D} = \{a_1, \dots, a_T\} \sim \pi_h^\beta(\cdot | s)$ , and a  $\mathcal{N}(0, I)$  prior on  $\mu_h(s)$ . Our theory suggests that instead of fitting the BC policy, we should fit the posterior demonstrator policy  $\hat{\pi}^{\text{post}}$ . In this Gaussian setting, it is straightforward to show that  $\hat{\pi}_h^{\text{post}}(\cdot | s)$  is the distribution:

$$\mathcal{N}\left(\frac{1}{\sigma_h^2(s)+T} \cdot \sum_{t=1}^T a_t, \frac{\sigma_h^2(s)}{\sigma_h^2(s)+T} \cdot I + \sigma_h^2(s) \cdot I\right).$$

While in the Gaussian setting we can easily sample from this distribution, we wish to motivate a generalizable procedure that extends to settings where sampling is less straightforward. To this end, we first note that the BC policy (the MAP estimator) is simply the distribution

$$\mathcal{N}\left(\frac{1}{\sigma_h^2(s)+T} \cdot \sum_{t=1}^T a_t, \sigma_h^2(s) \cdot I\right).$$

To generate a sample from  $\hat{\pi}_h^{\text{post}}(\cdot | s)$ , it then suffices to sample from the BC policy and perturb the sample by noise  $w \sim \mathcal{N}(0, \frac{\sigma_h^2(s)}{\sigma_h^2(s)+T} \cdot I)$ . The following result, an extension of Osband et al. (2018), shows that there is a close connection between this noise distribution and the posterior on  $\mu_h(s)$ , and that we can generate a sample from the posterior on  $\mu_h(s)$  with a simple optimization procedure.

**Proposition 4.** *We have  $P_{\text{post}}^\beta(\cdot | \mathfrak{D}) = \mathcal{N}(\frac{1}{\sigma_h^2(s)+T} \cdot \sum_{t=1}^T a_t, \frac{\sigma_h^2(s)}{\sigma_h^2(s)+T} \cdot I)$  and, if we set*

$$\hat{\mu}_h(s) = \arg \min_{\mu} \sum_{i=1}^T \|\mu - \tilde{a}_i\|_2^2 + \sigma_h^2(s) \cdot \|\mu - \tilde{\mu}_h(s)\|_2^2,$$

*for  $\tilde{a}_t = a_t + w_t$ ,  $w_t \sim \mathcal{N}(0, \sigma_h^2(s) \cdot I)$ , and  $\tilde{\mu}_h(s) \sim \mathcal{N}(0, I)$ , then  $\hat{\mu}_h(s) \sim P_{\text{post}}^\beta(\cdot | \mathfrak{D})$ .*

Thus, to generate a sample  $w \sim \mathcal{N}(0, \frac{\sigma_h^2(s)}{\sigma_h^2(s)+T} \cdot I)$ , we can first generate samples  $\hat{\mu}_h(s)$ , compute their empirical variance, which we denote as  $\text{cov}_h(s)$ , and sample from a Gaussian with mean 0 and variance  $\text{cov}_h(s)$ . Altogether, then, we have the following procedure to sample  $\hat{a} \sim \hat{\pi}_h^{\text{post}}(\cdot | s)$ :

1. Compute the BC policy  $\hat{\pi}^{\text{bc}}$  from observations  $\mathfrak{D}$ .
2. Compute samples from the posterior  $P_{\text{post}}^\beta$  using the optimization procedure of Proposition 4, and estimate the variance  $\text{cov}_h(s)$  of the posterior from these samples.
3. Generate samples  $\tilde{a} \sim \hat{\pi}_h^{\text{bc}}(\cdot | s)$  and  $w \sim \mathcal{N}(0, \text{cov}_h(s))$ , and set  $\hat{a} \leftarrow \tilde{a} + w$ .

While in the Gaussian setting simpler methods would suffice to generate a sample from  $\hat{\pi}^{\text{post}}$ , critically, each step in this procedure can be easily extended to more complex settings, suggesting a generalizable approach to approximate samples from  $\hat{\pi}^{\text{post}}$ .

## 5.2 Practical Instantiation of Posterior Behavioral Cloning

In practice our data likely does not satisfy the above Gaussianity assumption, and we also wish to incorporate function approximation to handle settings where we do not have multiple samples from the same state. In this section we show how the above procedure motivates a general approach to sample from  $\hat{\pi}^{\text{post}}$  in such settings. First, to generate approximate samples from  $P_{\text{post}}^\beta$ , we generalize the optimization-based procedure of Proposition 4 to the following.

---

### Algorithm 1 Posterior Variance Approximation via Ensembled Prediction

---

- 1: **input:** demonstration dataset  $\mathfrak{D}$ , ensemble size  $K$ , posterior model class  $\mathcal{F}$
- 2: **for**  $\ell = 1, 2, \dots, K$  **do**
- 3:     Set  $\mathfrak{D}_\ell$  to “noisy” version of  $\mathfrak{D}$
- 4:     Fit  $f_\ell$  by solving  $f_\ell \leftarrow \arg \min_{f \in \mathcal{F}} \sum_{(s, \tilde{a}) \in \mathfrak{D}_\ell} \|f_\ell(s) - \tilde{a}\|_2^2$
- 5:      $\text{cov}(\cdot) \leftarrow \sum_{\ell=1}^K (f_\ell(\cdot) - \bar{f}(\cdot))(f_\ell(\cdot) - \bar{f}(\cdot))^\top$  for  $\bar{f}(\cdot) \leftarrow \frac{1}{K} \sum_{\ell=1}^K f_\ell(\cdot)$

---

Algorithm 1 fits an ensemble of predictors to a perturbed version of  $\mathfrak{D}$  in order to approximate a posterior sample, and uses these samples to approximate the posterior covariance. While these samples may not correspond precisely to the posterior covariance in general settings, Proposition 4 shows that in simple settings they do, suggesting that, at minimum, this is a principled approximation. In the Gaussian setting we generate a noisy  $\mathfrak{D}$  by perturbing the actions in  $\mathfrak{D}$  with Gaussian noise. In practice, however, other methods to obtain a “noisy” version of  $\mathfrak{D}$  can be applied as well. In particular, we found that generating  $\mathfrak{D}_\ell$  by *bootstrapped sampling* (Fushiki et al., 2005; Osband & Van Roy, 2015; Osband et al., 2016a)—where we sample with replacement from  $\mathfrak{D}$ —typically outperforms directly adding noise to the actions in  $\mathfrak{D}$ .

Given the approximate posterior covariance  $\text{cov}(\cdot)$ , Section 5.1 suggests that for any  $s$  we can generate approximate samples from  $\hat{\pi}^{\text{post}}(\cdot | s)$  by first sampling an action from the BC policy at  $s$ , and then perturbing the resulting action by posterior noise  $w \sim \mathcal{N}(0, \text{cov}(s))$ . In practice, to avoid this two-stage procedure, we can fit a single policy to  $\mathfrak{D}$  (which would be the BC policy) but where we perturb each action in  $\mathfrak{D}$  by the posterior noise. Note that the distribution this policy will fit is equivalent to the distribution produced by the above two-stage procedure, as long as we utilize an expressive generative model able to represent the posterior demonstrator policy. We arrive at the following.

---

**Algorithm 2** Posterior Behavioral Cloning (POSTBC)

---

```

1: input: demonstration dataset  $\mathfrak{D}$ , generative model class  $\hat{\pi}^\theta$ , posterior covariance  $\text{cov}(\cdot)$ , posterior weight  $\alpha$ 
2: for  $i = 1, 2, 3, \dots$  do
3:   Sample batch  $\mathfrak{B}_i \sim \text{unif}(\mathfrak{D})$ 
4:   For all  $(s, a) \in \mathfrak{B}_i$ , sample  $w_s \sim \mathcal{N}(0, \text{cov}(s))$ , and set  $\tilde{\mathfrak{B}}_i \leftarrow \{(s, a + \alpha \cdot w_s) : s \in \mathfrak{B}_i\}$ 
5:   Take gradient step on  $\hat{\pi}^\theta$  for loss computed on  $\tilde{\mathfrak{B}}_i$ 
6: return  $\hat{\pi}^\theta$ 

```

---

Altogether, if  $\hat{\pi}^\theta$  is an expressive generative model, Algorithm 2 will produce a policy that, instead of fitting the empirical distribution of the demonstrator as BC does, fits the full posterior demonstrator policy. This approximates the posterior mixture in Equation (2), and, Theorem 1 suggests, leads to a more effective initialization for RL finetuning, instantiating the behavior illustrated in Figure 1. As Theorem 1 suggests that instead of sampling just from  $\hat{\pi}^{\text{post}}$  we should sample from a mixture of  $\hat{\pi}^{\text{post}}$  and  $\hat{\pi}^{\text{bc}}$ , Algorithm 2 modulates the weight of the posterior noise by some  $\alpha$ , allowing us to vary the weight of the mixture by varying  $\alpha$ .

Furthermore, Algorithm 1 can be implemented with standard supervised learning training pipelines (it requires only standard regression training), and implementing Algorithm 2 only requires minor modification to standard generative policy training (simply add noise to the action target for each batch sampled). POSTBC then only requires training via standard supervised learning—no RL in pretraining is required—making it a scalable approach and simple modification to existing BC training pipelines. While any expressive generative model class can be used for  $\hat{\pi}^\theta$ , in practice, for all the following experiments, we utilize a diffusion model. Please see Section D for further details on the practical instantiation of POSTBC.

## 6 Experiments

Finally, we seek to demonstrate that in practice POSTBC (a) enables more efficient RL finetuning of pretrained policies, and (b) produces a pretrained policy that itself performs effectively, on par with the BC pretrained policy. We focus on continuous control domains, in particular robotic control. We test on both the Robomimic (Mandlekar et al., 2021) and Libero (Liu et al., 2023) simulators (Sections 6.1 and 6.2), as well as a real-world WidowX 250 6-DoF robot arm (Section 6.3). We consider the Lift, Can, and Square tasks on Robomimic. Robomimic is comprised of several robotic manipulation tasks, provides a set of human demonstrations on each task, and enables training and finetuning of single-task BC policies. Libero

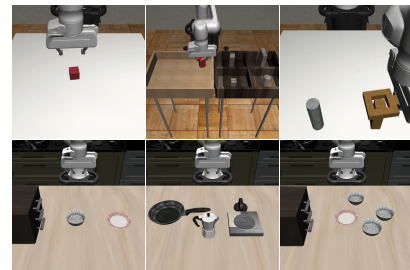


Figure 2: Robomimic and Libero settings

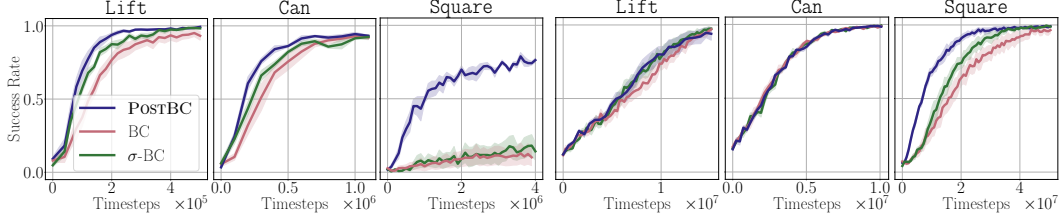


Figure 3: Comparison of DSRL finetuning performance combined with different BC pretraining approaches on Robomimic.

Figure 4: Comparison of DPPO finetuning performance combined with different BC pretraining approaches on Robomimic.

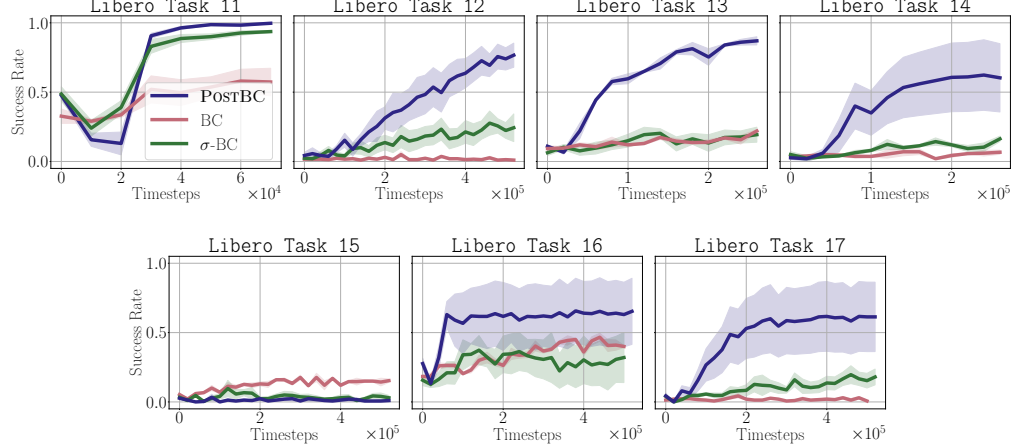


Figure 5: Comparison of DSRL finetuning performance combined with different BC pretraining approaches on all tasks from Libero 90, Kitchen Scene 2.

similarly contains a variety of robotic manipulation tasks with provided human demonstrations, but enables multi-task training, allowing for pretraining on large corpora of data and then finetuning on particular tasks of interest. In particular, we rely on a subset of the Libero 90 suite of tasks, training and evaluating on the scenes Kitchen Scene 1–3 containing a total of 16 tasks. See Figures 2 and 6 for visualizations of our settings. Further details on all experiments can be found in Section D.

We instantiate  $\hat{\pi}^{\text{pt}}$  with a diffusion model, a standard parameterization for BC policies in robotic control settings (Chi et al., 2023; Dasari et al., 2024; Team et al., 2024; Black et al., 2024; Bjork et al., 2025). For the Robomimic experiments, we use an MLP-based architecture, pretrain on a single-task demonstration dataset, and rely on state-based observations. For Libero, we utilize a diffusion transformer architecture due to Dasari et al. (2024) and rely on image-based observations and language task conditioning. In Libero, we pretrain a single  $\hat{\pi}^{\text{pt}}$  policy on the demonstration data from all 16 tasks (Black et al., 2024; Kim et al., 2024; Khazatsky et al., 2024), and then run RL finetuning on each individual task. On the WidowX experiments we utilize a U-Net architecture with image observations. In all cases, we use a binary success reward for the RL finetuning.

In principle, POSTBC can be combined with any RL finetuning algorithm, and we seek to demonstrate that it improves performance on a representative set of approaches. In particular, we consider DSRL (Wagenmaker et al., 2025a), which refines a pretrained diffusion policy’s distribution by running RL over its latent-noise space, DPPO (Ren et al., 2024), an on-policy policy-gradient-style algorithm for finetuning diffusion policies, and Best-of- $N$  sampling. For DSRL and DPPO we utilize the publicly available implementations without modification. Best-of- $N$  can be instantiated in a variety of ways (see e.g. Chen et al. (2022); Hansen-Estruch et al. (2023); He et al. (2024); Nakamoto et al. (2024); Dong et al. (2025b)). Here we instantiate it by rolling out the pretrained policy on the task of interest  $T_{\text{on}}$  times (where  $T_{\text{on}}$  is specified in our results) to collect trajectories labeled with success and failure, and train a  $Q$ -function via IQL (Kostrikov et al., 2021) on these trajectories. At test time, we again roll out the pretrained policy but at each state sample  $N$  actions from the policy, and play the action that has the largest value under this  $Q$ -function.

As baselines, we consider running standard BC pretraining on  $\mathfrak{D}$ , as well as what we refer to as  $\sigma$ -BC, where instead of perturbing the actions in  $\mathfrak{D}$  by the posterior variance as in Algorithm 2, we

Task	Best-of- $N$ (1000 Rollouts)				Best-of- $N$ (2000 Rollouts)			
	BC	$\sigma$ -BC	DICE	POSTBC	BC	$\sigma$ -BC	DICE	POSTBC
Robomimic Lift	59.4 $\pm$ 2.2	61.5 $\pm$ 3.9	44.4 $\pm$ 7.7	<b>74.2</b> $\pm$ 3.0	68.1 $\pm$ 2.2	<b>76.1</b> $\pm$ 3.5	47.6 $\pm$ 7.8	<b>81.3</b> $\pm$ 5.7
Robomimic Can	70.3 $\pm$ 1.7	<b>77.9</b> $\pm$ 1.2	17.0 $\pm$ 5.7	<b>75.0</b> $\pm$ 2.5	76.9 $\pm$ 1.5	<b>82.4</b> $\pm$ 1.6	41.8 $\pm$ 8.4	<b>84.5</b> $\pm$ 1.3
Robomimic Square	44.8 $\pm$ 0.7	48.1 $\pm$ 2.2	6.9 $\pm$ 0.9	<b>52.4</b> $\pm$ 1.9	<b>54.4</b> $\pm$ 1.3	<b>54.2</b> $\pm$ 3.7	8.3 $\pm$ 1.3	<b>56.8</b> $\pm$ 3.2
Libero Scene 1 (5 tasks)	37.7 $\pm$ 2.5	57.9 $\pm$ 3.4	-	<b>67.0</b> $\pm$ 5.6	46.1 $\pm$ 2.6	63.1 $\pm$ 4.1	-	<b>77.7</b> $\pm$ 1.3
Libero Scene 2 (7 tasks)	21.5 $\pm$ 1.2	26.9 $\pm$ 1.0	-	<b>42.0</b> $\pm$ 2.2	23.9 $\pm$ 0.7	29.0 $\pm$ 1.6	-	<b>49.5</b> $\pm$ 2.9
Libero Scene 3 (4 tasks)	47.7 $\pm$ 0.7	53.2 $\pm$ 2.3	-	<b>63.3</b> $\pm$ 5.1	45.8 $\pm$ 3.3	60.8 $\pm$ 1.9	-	<b>70.0</b> $\pm$ 0.4
Libero All (16 tasks)	33.1 $\pm$ 0.5	43.1 $\pm$ 0.8	-	<b>55.1</b> $\pm$ 2.1	36.3 $\pm$ 0.3	47.6 $\pm$ 2.8	-	<b>63.4</b> $\pm$ 1.3

Table 1: Comparison of success rates of pretrained policies and Best-of- $N$  sampling on Robomimic and Libero, for different pretraining approaches. Bolded text denotes best approach.

instead perturb them by uniform, state-independent noise with variance  $\sigma^2$ . This is then equivalent to POSTBC, except we set  $\text{cov}(s) = \sigma^2 \cdot I$  for some fixed  $\sigma > 0$  in Algorithm 2 (note that this is a continuous analog to the approach considered in Proposition 3). This itself is a novel approach and our theory predicts it too may lead to improved performance over pretraining with standard BC. On Robomimic, we also compare against VALUEDICE (Kostrikov et al., 2019) (which we abbreviate as DICE), as a representative non-BC imitation learning approach. Rather than training to match the demonstrator’s actions via supervised learning, VALUEDICE attempts to learn a policy with state distribution matching the state distribution of the demonstrations, and only requires access to offline demonstration data. All Robomimic results are averaged over 5 seeds, and Libero results are averaged over 3 seeds, and policies are evaluated with 200 rollouts for Robomimic and 100 for Libero. For all experiments, error bars denote 1 standard error.

## 6.1 Posterior Behavioral Cloning Enables Efficient RL Finetuning

Our results from running DSRL on Robomimic are given in Figure 3 and on Libero in Figure 5. On Robomimic, POSTBC significantly outperforms both baselines on Square, and achieves modest gains over BC on Lift and Can (requiring roughly 2 $\times$  fewer samples to achieve 75% performance than BC). For Libero, we run DSRL on all tasks from Kitchen Scene 2. We see that POSTBC pretraining leads to significant gains for Libero, enabling efficient RL finetuning in settings where both standard BC pretraining and  $\sigma$ -BC pretraining fail. Our results for DPPO are given in Figure 3 where we see that POSTBC pretraining again leads to substantial gains on Square (again approximately 2 $\times$  fewer samples to reach 75% performance compared to BC). This illustrates that POSTBC still improves performance even for RL finetuning algorithms that modify the weights of the pretrained policy, and for which the resulting actions are therefore not explicitly constrained to the actions played by the pretrained policy. Our Best-of- $N$  results are given in Table 1. We see that across settings, POSTBC-pretraining leads to consistent improvements over both BC- and  $\sigma$ -BC-pretrained policies for Best-of- $N$ , and also consistently outperforms VALUEDICE. In particular, on Libero, POSTBC improves by approximately 20-30% over BC, and 10-20% over  $\sigma$ -BC. We note as well that, even in the cases when POSTBC does not yield substantial gains, it performs no worse than BC. These results illustrate that POSTBC enables more effective RL finetuning on both single-task settings (for each Robomimic task we pretrain a single policy) as well as multi-task settings (for Libero we pretrain a single policy across tasks), and across state- and image-based observations.

## 6.2 Posterior Behavioral Cloning Preserves Pretrained Performance

We next show that POSTBC pretraining produces a policy that has pretrained performance no worse than that of the BC-pretrained policy. We provide results on pretrained performance for Robomimic and Libero in Table 2. As these results illustrate, across both single-task and multi-task settings, the POSTBC policy performs comparably to, or even better than, the BC policy in terms of pretrained performance. In contrast, the  $\sigma$ -BC policy often suffers from marginally lower performance than the BC policy (while also underperforming the POSTBC policy in terms of finetuned performance), and the VALUEDICE policy

Task	Pretrained Performance			
	BC	$\sigma$ -BC	DICE	POSTBC
Robomimic Lift	<b>71.0</b> $\pm$ 0.5	68.0 $\pm$ 0.7	25.5 $\pm$ 4.4	<b>69.7</b> $\pm$ 1.5
Robomimic Can	<b>43.1</b> $\pm$ 0.9	42.3 $\pm$ 0.8	14.2 $\pm$ 2.5	<b>44.7</b> $\pm$ 1.0
Robomimic Square	<b>17.9</b> $\pm$ 0.7	<b>17.8</b> $\pm$ 0.7	5.7 $\pm$ 0.3	<b>18.1</b> $\pm$ 0.8
Libero Scene 1 (5 tasks)	<b>23.6</b> $\pm$ 1.7	<b>22.3</b> $\pm$ 2.1	-	<b>25.3</b> $\pm$ 1.2
Libero Scene 2 (7 tasks)	<b>11.4</b> $\pm$ 0.2	<b>10.6</b> $\pm$ 0.8	-	<b>12.3</b> $\pm$ 1.5
Libero Scene 3 (4 tasks)	<b>39.5</b> $\pm$ 1.5	36.9 $\pm$ 1.8	-	<b>40.8</b> $\pm$ 1.3
Libero All (16 tasks)	22.2 $\pm$ 0.3	20.9 $\pm$ 0.6	-	<b>23.5</b> $\pm$ 0.5

Table 2: Comparison of success rates of all pretrained policies on Robomimic and Libero, for different pretraining approaches. Bolded text denotes best approach.



Figure 6: WidowX setup.

Task	Pretrained Performance		Best-of- $N$ (100 Rollouts)	
	BC	POSTBC	BC	POSTBC
Pick up banana	2/20	<b>4/20</b>	10/20	<b>16/20</b>
Put corn in pot	3/20	<b>7/20</b>	5/20	<b>13/20</b>

Table 3: Comparison of BC and POSTBC on real-world WidowX tasks using Best-of- $N$  sampling. We see that POSTBC enables significantly larger improvement than BC, while also improving the success rate of the pretrained policy.

significantly underperforms all BC policies. Combined with the results of Section 6.1, this shows that POSTBC not only enables more effective RL finetuning, it does this without hurting the performance of the pretrained policy.

### 6.3 Posterior Behavioral Cloning Scales to Real-World Robotic Manipulation

We next show that POSTBC scales to real-world robotic settings, leading to improvement in real-world RL finetuning over standard BC pretraining. We evaluate on the WidowX 250 6-DoF robot arm and consider two tasks on the scene illustrated in Figure 6. We first collect 10 human teleoperation demonstrations for the task “Put corn in pot”, where the objective is to pick up the corn and set it in the pot. We train diffusion policies with standard BC as well as POSTBC on these demonstrations. For RL finetuning we consider two tasks—the original “Put corn in pot” task the policy is trained on, and the task “Pick up banana” where the corn is replaced with a banana and the goal of the robot is to simply pick up the banana (see Figure 11). For RL finetuning, we consider the Best-of- $N$  procedure outlined above, and utilize 100 rollouts per task.

Our results are given in Table 3. We see that POSTBC leads to significant improvements over BC—in both tasks achieving significantly higher final success rate. In particular, for the “Put corn in pot” task, RL finetuning is only able to marginally improve the performance of the BC policy—a 10% improvement in success rate from the base policy—while the POSTBC policy improves by 30%. Furthermore, POSTBC pretraining not only does not hurt the success rate of the pretrained policy, but actually leads to improved performance of the pretrained policy. This illustrates that POSTBC scales to real robot settings, providing improved RL finetuning performance without decreasing pretrained policy performance.

### 6.4 Understanding Posterior Behavioral Cloning

Finally, we seek to provide insight into how POSTBC improves RL finetuning performance. We first aim to disambiguate the role of the additional exploration a POSTBC policy may provide over a BC policy, versus the role that having access to a larger action distribution at test time might play. While these factors are intimately coupled for DSRL and DPPO, for Best-of- $N$  sampling we can decouple them by selecting the rollout policy (the “exploration” policy) that collects data to learn the  $Q$ -function with IQL, and the policy whose actions we sample from and filter with the learned  $Q$ -function at test-time (the “test-time” policy).

We consider mixing the role of the BC and POSTBC policy on Robomimic Lift in this way, and provide our results in Table 4. We find that using POSTBC as the test-time policy is critical to achieving effective performance, but that this performance is achievable whether we use BC or POSTBC for the exploration policy. This suggests that the utility of POSTBC is primarily in its ability to provide a wider range of actions that can be sampled from the pretrained policy at test time, enabling RL finetuning approaches to easily select the best action.

Next we consider the qualitative behavior of the POSTBC pretrained policy compared to the BC and  $\sigma$ -BC policies. We illustrate this on Libero task “Open the top drawer of the cabinet and put the bowl in it” and display a heatmap of the visitations for each policy in Figure 7 (please see Section D.4 for visualizations on additional tasks). We see that POSTBC exhibits the widest

BC exploration + BC test-time	BC exploration + POSTBC test-time	POSTBC exploration + BC test-time	POSTBC exploration + POSTBC test-time
$68.1 \pm 2.2$	<b><math>82.7 \pm 1.9</math></b>	$29.4 \pm 3.6$	<b><math>81.3 \pm 5.7</math></b>

Table 4: Best-of- $N$  sampling on Robomimic Lift with 2000 rollouts, varying the exploration policy and the test-time policy.

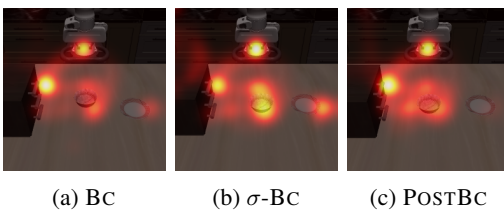


Figure 7: Qualitative analysis of POSTBC on Libero task “Open the top drawer of the cabinet and put the bowl in it”.

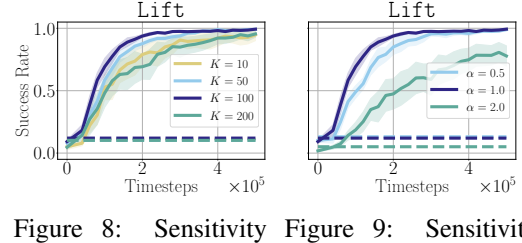


Figure 8: Sensitivity of POSTBC with DSRL finetuning to ensemble size. Dashed lines denote pretrained policy performance.

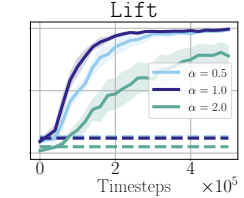


Figure 9: Sensitivity of POSTBC with DSRL finetuning to posterior weight. Dashed lines denote pretrained policy performance.

distribution of states around the bowl, ensuring that it covers the behaviors necessary to reliably pick up the bowl, the most challenging aspect of this task. In contrast, BC and  $\sigma$ -BC exhibit less diversity around the bowl, which, if they do not cover all behaviors necessary to effectively pick up the bowl, may make them more difficult to finetune. At the same time, while exhibiting diversity around the states relevant to the task, POSTBC focuses its behavior only on these relevant behaviors, ensuring the pretrained policy still performs effectively. In contrast,  $\sigma$ -BC also interacts with the plate, which is irrelevant to this task and would therefore hurt its pretrained performance.

Finally, we consider the sensitivity of POSTBC to two key hyperparameters: the size of the ensemble ( $K$ ) and the weight of the posterior variance ( $\alpha$  in Algorithm 2). We illustrate the performance of POSTBC on Robomimic Lift varying these parameters in Figures 8 and 9. In Figure 8 we see that POSTBC performs best with a moderately sized ensemble ( $K = 100$ ), but is not particularly sensitive to ensemble size as long as it is not too small or too large. In Figure 9 we see that setting  $\alpha$  too large can hurt the performance of POSTBC, but that otherwise the performance of POSTBC is relatively stable with respect to  $\alpha$ . We note as well that setting  $\alpha$  too large not only hurts the performance of the RL finetuning, but also causes the pretrained performance to drop. This is to be expected—even with the carefully tuned noise POSTBC adds to the policy in pretraining, if the weight of this noise is too large the perturbations it induces will cause performance to drop below that of the BC policy. In general, throughout our experiments, we found that  $\alpha = 1$  typically performs well.

## 7 Conclusion

In this work, we have proposed a novel approach to pretraining policies from demonstrations that ensures the pretrained performance is no worse than that of the BC policy, while expanding the action distribution to enable more effective RL finetuning. We have shown that this approach does indeed lead to improved RL finetuning performance in practice, scaling to real-world robotic settings. We believe this work motivates a variety of interesting questions for future work.

- Our demonstrator action coverage condition introduced in Section 4.1 is a *necessary* condition, in some cases, for RL finetuning to reach the performance of the demonstrator policy, as Proposition 2 shows. In general, however, demonstrator action coverage does not give a guarantee about the sample complexity of the downstream RL finetuning. Can we derive a non-trivial *sufficient* condition that ensures efficient RL finetuning without the aid of exploration approaches typically absent in practice (such as optimism), and how can we pretrain policies to ensure they meet such a sufficient condition?
- We have focused on pretraining only with supervised learning. While this is the most scalable approach, and the most commonly used approach in practice, is this a limiting factor in obtaining an effective initialization for online RL finetuning, and could we pretrain using other approaches as well (for example, offline RL)?
- While we have primarily considered applications to robotic control, our approach could also be applied in language domains. Does pretraining (or SFT finetuning) of language models with our approach lead to improved performance in downstream RL finetuning?

## Acknowledgments

This research was partly supported by RAI, ONR N00014-25-1-2060, and NSF IIS-2150826. The work of CF was partially supported by an NSF CAREER award.

## References

Pieter Abbeel and Andrew Y Ng. Apprenticeship learning via inverse reinforcement learning. In *Proceedings of the twenty-first international conference on Machine learning*, pp. 1, 2004.

Shipra Agrawal and Navin Goyal. Analysis of thompson sampling for the multi-armed bandit problem. In *Conference on learning theory*, pp. 39–1. JMLR Workshop and Conference Proceedings, 2012.

Lars Ankile, Anthony Simeonov, Idan Shenfeld, and Pulkit Agrawal. Juicer: Data-efficient imitation learning for robotic assembly. In *2024 IEEE/RSJ International Conference on Intelligent Robots and Systems (IROS)*, pp. 5096–5103. IEEE, 2024a.

Lars Ankile, Anthony Simeonov, Idan Shenfeld, Marcel Torne, and Pulkit Agrawal. From imitation to refinement–residual rl for precise assembly. *arXiv preprint arXiv:2407.16677*, 2024b.

Mohammad Gheshlaghi Azar, Zhaoan Daniel Guo, Bilal Piot, Remi Munos, Mark Rowland, Michal Valko, and Daniele Calandriello. A general theoretical paradigm to understand learning from human preferences. In *International Conference on Artificial Intelligence and Statistics*, pp. 4447–4455. PMLR, 2024.

Yuntao Bai, Andy Jones, Kamal Ndousse, Amanda Askell, Anna Chen, Nova DasSarma, Dawn Drain, Stanislav Fort, Deep Ganguli, Tom Henighan, et al. Training a helpful and harmless assistant with reinforcement learning from human feedback. *arXiv preprint arXiv:2204.05862*, 2022a.

Yuntao Bai, Saurav Kadavath, Sandipan Kundu, Amanda Askell, Jackson Kernion, Andy Jones, Anna Chen, Anna Goldie, Azalia Mirhoseini, Cameron McKinnon, et al. Constitutional ai: Harmlessness from ai feedback. *arXiv preprint arXiv:2212.08073*, 2022b.

Michiel Bakker, Martin Chadwick, Hannah Sheahan, Michael Tessler, Lucy Campbell-Gillingham, Jan Balaguer, Nat McAleese, Amelia Glaese, John Aslanides, Matt Botvinick, et al. Fine-tuning language models to find agreement among humans with diverse preferences. *Advances in Neural Information Processing Systems*, 35:38176–38189, 2022.

Philip J Ball, Laura Smith, Ilya Kostrikov, and Sergey Levine. Efficient online reinforcement learning with offline data. In *International Conference on Machine Learning*, pp. 1577–1594. PMLR, 2023.

Marc Bellemare, Sriram Srinivasan, Georg Ostrovski, Tom Schaul, David Saxton, and Remi Munos. Unifying count-based exploration and intrinsic motivation. *Advances in neural information processing systems*, 29, 2016.

Johan Bjorck, Fernando Castañeda, Nikita Cherniakov, Xingye Da, Runyu Ding, Linxi Fan, Yu Fang, Dieter Fox, Fengyuan Hu, Spencer Huang, et al. Gr0ot n1: An open foundation model for generalist humanoid robots. *arXiv preprint arXiv:2503.14734*, 2025.

Kevin Black, Noah Brown, Danny Driess, Adnan Esmail, Michael Equi, Chelsea Finn, Niccolo Fusai, Lachy Groom, Karol Hausman, Brian Ichter, et al.  $\pi_0$ : A vision-language-action flow model for general robot control. *arXiv preprint arXiv:2410.24164*, 2024.

Mariusz Bojarski. End to end learning for self-driving cars. *arXiv preprint arXiv:1604.07316*, 2016.

Yuri Burda, Harrison Edwards, Amos Storkey, and Oleg Klimov. Exploration by random network distillation. *arXiv preprint arXiv:1810.12894*, 2018.

Jongseong Chae, Seungyul Han, Whiyoung Jung, Myungsik Cho, Sungho Choi, and Youngchul Sung. Robust imitation learning against variations in environment dynamics. In *International Conference on Machine Learning*, pp. 2828–2852. PMLR, 2022.

Souradip Chakraborty, Jiahao Qiu, Hui Yuan, Alec Koppel, Furong Huang, Dinesh Manocha, Amit Singh Bedi, and Mengdi Wang. Maxmin-rlhf: Towards equitable alignment of large language models with diverse human preferences. *arXiv preprint arXiv:2402.08925*, 2024.

Jonathan D Chang, Wenhao Shan, Owen Oertell, Kianté Brantley, Dipendra Misra, Jason D Lee, and Wen Sun. Dataset reset policy optimization for rlhf. *arXiv preprint arXiv:2404.08495*, 2024.

Fan Chen, Audrey Huang, Noah Golowich, Sadhika Malladi, Adam Block, Jordan T Ash, Akshay Krishnamurthy, and Dylan J Foster. The coverage principle: How pre-training enables post-training. *arXiv preprint arXiv:2510.15020*, 2025a.

Feng Chen, Allan Raventos, Nan Cheng, Surya Ganguli, and Shaul Druckmann. Rethinking fine-tuning when scaling test-time compute: Limiting confidence improves mathematical reasoning. *arXiv preprint arXiv:2502.07154*, 2025b.

Huayu Chen, Cheng Lu, Chengyang Ying, Hang Su, and Jun Zhu. Offline reinforcement learning via high-fidelity generative behavior modeling. *arXiv preprint arXiv:2209.14548*, 2022.

Yuhui Chen, Shuai Tian, Shugao Liu, Yingting Zhou, Haoran Li, and Dongbin Zhao. Confft: A reinforced fine-tuning method for vla models via consistency policy. *arXiv preprint arXiv:2502.05450*, 2025c.

Cheng Chi, Zhenjia Xu, Siyuan Feng, Eric Cousineau, Yilun Du, Benjamin Burchfiel, Russ Tedrake, and Shuran Song. Diffusion policy: Visuomotor policy learning via action diffusion. *The International Journal of Robotics Research*, pp. 02783649241273668, 2023.

Jongwook Choi, Yijie Guo, Marcin Moczulski, Junhyuk Oh, Neal Wu, Mohammad Norouzi, and Honglak Lee. Contingency-aware exploration in reinforcement learning. *arXiv preprint arXiv:1811.01483*, 2018.

Sudeep Dasari and Abhinav Gupta. Transformers for one-shot visual imitation. In *Conference on Robot Learning*, pp. 2071–2084. PMLR, 2021.

Sudeep Dasari, Oier Mees, Sebastian Zhao, Mohan Kumar Srivama, and Sergey Levine. The ingredients for robotic diffusion transformers. *arXiv preprint arXiv:2410.10088*, 2024.

Siddharth Desai, Ishan Durugkar, Haresh Karnan, Garrett Warnell, Josiah Hanna, and Peter Stone. An imitation from observation approach to transfer learning with dynamics mismatch. *Advances in Neural Information Processing Systems*, 33:3917–3929, 2020.

Jacob Devlin, Ming-Wei Chang, Kenton Lee, and Kristina Toutanova. Bert: Pre-training of deep bidirectional transformers for language understanding. In *Proceedings of the 2019 conference of the North American chapter of the association for computational linguistics: human language technologies, volume 1 (long and short papers)*, pp. 4171–4186, 2019.

Perry Dong, Qiyang Li, Dorsa Sadigh, and Chelsea Finn. Expo: Stable reinforcement learning with expressive policies. *arXiv preprint arXiv:2507.07986*, 2025a.

Perry Dong, Suvir Mirchandani, Dorsa Sadigh, and Chelsea Finn. What matters for batch online reinforcement learning in robotics? *arXiv preprint arXiv:2505.08078*, 2025b.

Yan Duan, John Schulman, Xi Chen, Peter L Bartlett, Ilya Sutskever, and Pieter Abbeel. Rl<sup>2</sup>: Fast reinforcement learning via slow reinforcement learning. *arXiv preprint arXiv:1611.02779*, 2016.

Yan Duan, Marcin Andrychowicz, Bradly Stadie, OpenAI Jonathan Ho, Jonas Schneider, Ilya Sutskever, Pieter Abbeel, and Wojciech Zaremba. One-shot imitation learning. *Advances in neural information processing systems*, 30, 2017.

Vincent Dumoulin, Daniel D Johnson, Pablo Samuel Castro, Hugo Larochelle, and Yann Dauphin. A density estimation perspective on learning from pairwise human preferences. *arXiv preprint arXiv:2311.14115*, 2023.

Adrien Ecoffet, Joost Huizinga, Joel Lehman, Kenneth O Stanley, and Jeff Clune. Go-explore: a new approach for hard-exploration problems. *arXiv preprint arXiv:1901.10995*, 2019.

Chelsea Finn, Pieter Abbeel, and Sergey Levine. Model-agnostic meta-learning for fast adaptation of deep networks. In *International conference on machine learning*, pp. 1126–1135. PMLR, 2017a.

Chelsea Finn, Tianhe Yu, Tianhao Zhang, Pieter Abbeel, and Sergey Levine. One-shot visual imitation learning via meta-learning. In *Conference on robot learning*, pp. 357–368. PMLR, 2017b.

Chelsea Finn, Kelvin Xu, and Sergey Levine. Probabilistic model-agnostic meta-learning. *Advances in neural information processing systems*, 31, 2018.

Dylan J Foster, Sham M Kakade, Jian Qian, and Alexander Rakhlin. The statistical complexity of interactive decision making. *arXiv preprint arXiv:2112.13487*, 2021.

Justin Fu, Katie Luo, and Sergey Levine. Learning robust rewards with adversarial inverse reinforcement learning. *arXiv preprint arXiv:1710.11248*, 2017.

Tadayoshi Fushiki, Fumiyasu Komaki, and Kazuyuki Aihara. Nonparametric bootstrap prediction. *Bernoulli*, 11(2):293–307, 2005.

Chongkai Gao, Yizhou Jiang, and Feng Chen. Transferring hierarchical structures with dual meta imitation learning. In *Conference on Robot Learning*, pp. 762–773. PMLR, 2023.

Divyansh Garg, Shuvam Chakraborty, Chris Cundy, Jiaming Song, and Stefano Ermon. Iq-learn: Inverse soft-q learning for imitation. *Advances in Neural Information Processing Systems*, 34: 4028–4039, 2021.

Divya Ghosh, Anurag Ajay, Pulkit Agrawal, and Sergey Levine. Offline rl policies should be trained to be adaptive. In *International Conference on Machine Learning*, pp. 7513–7530. PMLR, 2022.

Vittorio Gammariello, James Queeney, and Ioannis Ch Paschalidis. Visually robust adversarial imitation learning from videos with contrastive learning. In *2025 IEEE International Conference on Robotics and Automation (ICRA)*, pp. 15642–15648. IEEE, 2025.

Jiayuan Gu, Sean Kirmani, Paul Wohlhart, Yao Lu, Montserrat Gonzalez Arenas, Kanishka Rao, Wenhao Yu, Chuyuan Fu, Keerthana Gopalakrishnan, Zhuo Xu, et al. Rt-trajectory: Robotic task generalization via hindsight trajectory sketches. *arXiv preprint arXiv:2311.01977*, 2023.

Daya Guo, Dejian Yang, Haowei Zhang, Junxiao Song, Ruoyu Zhang, Runxin Xu, Qihao Zhu, Shirong Ma, Peiyi Wang, Xiao Bi, et al. Deepseek-r1: Incentivizing reasoning capability in llms via reinforcement learning. *arXiv preprint arXiv:2501.12948*, 2025a.

Yanjiang Guo, Jianke Zhang, Xiaoyu Chen, Xiang Ji, Yen-Jen Wang, Yucheng Hu, and Jianyu Chen. Improving vision-language-action model with online reinforcement learning. *arXiv preprint arXiv:2501.16664*, 2025b.

Philippe Hansen-Estruch, Ilya Kostrikov, Michael Janner, Jakub Grudzien Kuba, and Sergey Levine. Idql: Implicit q-learning as an actor-critic method with diffusion policies. *arXiv preprint arXiv:2304.10573*, 2023.

Longxiang He, Li Shen, Junbo Tan, and Xueqian Wang. Alignql: Policy alignment in implicit q-learning through constrained optimization. *arXiv preprint arXiv:2405.18187*, 2024.

Mikael Henaff, Roberta Raileanu, Minqi Jiang, and Tim Rocktäschel. Exploration via elliptical episodic bonuses. *Advances in Neural Information Processing Systems*, 35:37631–37646, 2022.

Jonathan Ho and Stefano Ermon. Generative adversarial imitation learning. *Advances in neural information processing systems*, 29, 2016.

Jonathan Ho, Ajay Jain, and Pieter Abbeel. Denoising diffusion probabilistic models. *Advances in neural information processing systems*, 33:6840–6851, 2020.

Hao Hu, Yiqin Yang, Jianing Ye, Ziqing Mai, and Chongjie Zhang. Unsupervised behavior extraction via random intent priors. *Advances in Neural Information Processing Systems*, 36:51491–51514, 2023.

Jiaheng Hu, Rose Hendrix, Ali Farhadi, Aniruddha Kembhavi, Roberto Martín-Martín, Peter Stone, Kuo-Hao Zeng, and Kiana Ehsani. Flare: Achieving masterful and adaptive robot policies with large-scale reinforcement learning fine-tuning. In *2025 IEEE International Conference on Robotics and Automation (ICRA)*, pp. 3617–3624. IEEE, 2025.

Stephen James, Michael Bloesch, and Andrew J Davison. Task-embedded control networks for few-shot imitation learning. In *Conference on robot learning*, pp. 783–795. PMLR, 2018.

David Janz, Shuai Liu, Alex Ayoub, and Csaba Szepesvári. Exploration via linearly perturbed loss minimisation. In *International Conference on Artificial Intelligence and Statistics*, pp. 721–729. PMLR, 2024.

Hangzhan Jin, Sitao Luan, Sicheng Lyu, Guillaume Rabusseau, Reihaneh Rabbany, Doina Precup, and Mohammad Hamdaqa. Rl fine-tuning heals ood forgetting in sft. *arXiv preprint arXiv:2509.12235*, 2025.

Tobias Jülg, Wolfram Burgard, and Florian Walter. Refined policy distillation: From vla generalists to rl experts. *arXiv preprint arXiv:2503.05833*, 2025.

Alexander Khazatsky, Karl Pertsch, Suraj Nair, Ashwin Balakrishna, Sudeep Dasari, Siddharth Karamchetti, Soroush Nasiriany, Mohan Kumar Srirama, Lawrence Yunliang Chen, Kirsty Ellis, Peter David Fagan, Joey Hejna, Masha Itkina, Marion Lepert, Yecheng Jason Ma, Patrick Tree Miller, Jimmy Wu, Suneel Belkhale, Shivin Dass, Huy Ha, Arhan Jain, Abraham Lee, Young-woon Lee, Marius Memmel, Sungjae Park, Ilija Radosavovic, Kaiyuan Wang, Albert Zhan, Kevin Black, Cheng Chi, Kyle Beltran Hatch, Shan Lin, Jingpei Lu, Jean Mercat, Abdul Rehman, Pannag R Sanketi, Archit Sharma, Cody Simpson, Quan Vuong, Homer Rich Walke, Blake Wulfe, Ted Xiao, Jonathan Heewon Yang, Arefeh Yavary, Tony Z. Zhao, Christopher Agia, Rohan Baijal, Mateo Guaman Castro, Daphne Chen, Qiuyu Chen, Trinity Chung, Jaimyn Drake, Ethan Paul Foster, Jensen Gao, Vitor Guizilini, David Antonio Herrera, Minho Heo, Kyle Hsu, Jiaheng Hu, Muhammad Zubair Irshad, Donovon Jackson, Charlotte Le, Yunshuang Li, Kevin Lin, Roy Lin, Zehan Ma, Abhiram Maddukuri, Suvir Mirchandani, Daniel Morton, Tony Nguyen, Abigail O'Neill, Rosario Scalise, Derick Seale, Victor Son, Stephen Tian, Emi Tran, Andrew E. Wang, Yilin Wu, Annie Xie, Jingyun Yang, Patrick Yin, Yunchu Zhang, Osbert Bastani, Glen Berseth, Jeannette Bohg, Ken Goldberg, Abhinav Gupta, Abhishek Gupta, Dinesh Jayaraman, Joseph J Lim, Jitendra Malik, Roberto Martín-Martín, Subramanian Ramamoorthy, Dorsa Sadigh, Shuran Song, Jiajun Wu, Michael C. Yip, Yuke Zhu, Thomas Kollar, Sergey Levine, and Chelsea Finn. *Droid: A large-scale in-the-wild robot manipulation dataset*. 2024.

Moo Jin Kim, Karl Pertsch, Siddharth Karamchetti, Ted Xiao, Ashwin Balakrishna, Suraj Nair, Rafael Rafailov, Ethan Foster, Grace Lam, Pannag Sanketi, et al. *Openvla: An open-source vision-language-action model*. *arXiv preprint arXiv:2406.09246*, 2024.

Moo Jin Kim, Chelsea Finn, and Percy Liang. Fine-tuning vision-language-action models: Optimizing speed and success. *arXiv preprint arXiv:2502.19645*, 2025.

Ilya Kostrikov, Kumar Krishna Agrawal, Debidatta Dwibedi, Sergey Levine, and Jonathan Tompson. Discriminator-actor-critic: Addressing sample inefficiency and reward bias in adversarial imitation learning. *arXiv preprint arXiv:1809.02925*, 2018.

Ilya Kostrikov, Ofir Nachum, and Jonathan Tompson. Imitation learning via off-policy distribution matching. *arXiv preprint arXiv:1912.05032*, 2019.

Ilya Kostrikov, Ashvin Nair, and Sergey Levine. Offline reinforcement learning with implicit q-learning. *arXiv preprint arXiv:2110.06169*, 2021.

Aviral Kumar, Anikait Singh, Frederik Ebert, Mitsuhiro Nakamoto, Yanlai Yang, Chelsea Finn, and Sergey Levine. Pre-training for robots: Offline rl enables learning new tasks from a handful of trials. *arXiv preprint arXiv:2210.05178*, 2022.

Branislav Kveton, Manzil Zaheer, Csaba Szepesvari, Lihong Li, Mohammad Ghavamzadeh, and Craig Boutilier. Randomized exploration in generalized linear bandits. In *International Conference on Artificial Intelligence and Statistics*, pp. 2066–2076. PMLR, 2020.

Harrison Lee, Samrat Phatale, Hassan Mansoor, Kellie Lu, Thomas Mesnard, Colton Bishop, Victor Carbune, and Abhinav Rastogi. Rlaif: Scaling reinforcement learning from human feedback with ai feedback. *arXiv preprint arXiv:2309.00267*, 2023.

Kimin Lee, Michael Laskin, Aravind Srinivas, and Pieter Abbeel. Sunrise: A simple unified framework for ensemble learning in deep reinforcement learning. In *International Conference on Machine Learning*, pp. 6131–6141. PMLR, 2021.

Seunghyun Lee, Younggyo Seo, Kimin Lee, Pieter Abbeel, and Jinwoo Shin. Offline-to-online reinforcement learning via balanced replay and pessimistic q-ensemble. In *Conference on Robot Learning*, pp. 1702–1712. PMLR, 2022.

Qiyang Li, Jason Zhang, Dibya Ghosh, Amy Zhang, and Sergey Levine. Accelerating exploration with unlabeled prior data. *Advances in Neural Information Processing Systems*, 36:67434–67458, 2023a.

Ziniu Li, Tian Xu, Zeyu Qin, Yang Yu, and Zhi-Quan Luo. Imitation learning from imperfection: Theoretical justifications and algorithms. *Advances in Neural Information Processing Systems*, 36:18404–18443, 2023b.

Bo Liu, Yifeng Zhu, Chongkai Gao, Yihao Feng, Qiang Liu, Yuke Zhu, and Peter Stone. Libero: Benchmarking knowledge transfer for lifelong robot learning. *Advances in Neural Information Processing Systems*, 36:44776–44791, 2023.

Jijia Liu, Feng Gao, Bingwen Wei, Xinlei Chen, Qingmin Liao, Yi Wu, Chao Yu, and Yu Wang. What can rl bring to vla generalization? an empirical study. *arXiv preprint arXiv:2505.19789*, 2025.

Guanxing Lu, Wenkai Guo, Chubin Zhang, Yuheng Zhou, Haonan Jiang, Zifeng Gao, Yansong Tang, and Ziwei Wang. Vla-rl: Towards masterful and general robotic manipulation with scalable reinforcement learning. *arXiv preprint arXiv:2505.18719*, 2025.

Ajay Mandlekar, Danfei Xu, Josiah Wong, Soroush Nasiriany, Chen Wang, Rohun Kulkarni, Li Fei-Fei, Silvio Savarese, Yuke Zhu, and Roberto Martín-Martín. What matters in learning from offline human demonstrations for robot manipulation. *arXiv preprint arXiv:2108.03298*, 2021.

Max Sobol Mark, Tian Gao, Georgia Gabriela Sampaio, Mohan Kumar Srirama, Archit Sharma, Chelsea Finn, and Aviral Kumar. Policy agnostic rl: Offline rl and online rl fine-tuning of any class and backbone. *arXiv preprint arXiv:2412.06685*, 2024.

Rémi Munos, Michal Valko, Daniele Calandriello, Mohammad Gheshlaghi Azar, Mark Rowland, Zhaohan Daniel Guo, Yunhao Tang, Matthieu Geist, Thomas Mesnard, Andrea Michi, et al. Nash learning from human feedback. *arXiv preprint arXiv:2312.00886*, 2023.

Mitsuhiko Nakamoto, Simon Zhai, Anikait Singh, Max Sobol Mark, Yi Ma, Chelsea Finn, Aviral Kumar, and Sergey Levine. Cal-ql: Calibrated offline rl pre-training for efficient online fine-tuning. *Advances in Neural Information Processing Systems*, 36:62244–62269, 2023.

Mitsuhiko Nakamoto, Oier Mees, Aviral Kumar, and Sergey Levine. Steering your generalists: Improving robotic foundation models via value guidance. *arXiv preprint arXiv:2410.13816*, 2024.

Andrew Y Ng, Stuart Russell, et al. Algorithms for inverse reinforcement learning. In *Icml*, volume 1, pp. 2, 2000.

Tianwei Ni, Harshit Sikchi, Yufei Wang, Tejas Gupta, Lisa Lee, and Ben Eysenbach. f-irl: Inverse reinforcement learning via state marginal matching. In *Conference on Robot Learning*, pp. 529–551. PMLR, 2021.

Ian Osband and Benjamin Van Roy. Bootstrapped thompson sampling and deep exploration. *arXiv preprint arXiv:1507.00300*, 2015.

Ian Osband, Charles Blundell, Alexander Pritzel, and Benjamin Van Roy. Deep exploration via bootstrapped dqn. *Advances in neural information processing systems*, 29, 2016a.

Ian Osband, Benjamin Van Roy, and Zheng Wen. Generalization and exploration via randomized value functions. In *International Conference on Machine Learning*, pp. 2377–2386. PMLR, 2016b.

Ian Osband, John Aslanides, and Albin Cassirer. Randomized prior functions for deep reinforcement learning. *Advances in neural information processing systems*, 31, 2018.

Long Ouyang, Jeffrey Wu, Xu Jiang, Diogo Almeida, Carroll Wainwright, Pamela Mishkin, Chong Zhang, Sandhini Agarwal, Katarina Slama, Alex Ray, et al. Training language models to follow instructions with human feedback. *Advances in neural information processing systems*, 35: 27730–27744, 2022.

Alec Radford, Karthik Narasimhan, Tim Salimans, Ilya Sutskever, et al. Improving language understanding by generative pre-training. 2018.

Rafael Rafailov, Archit Sharma, Eric Mitchell, Christopher D Manning, Stefano Ermon, and Chelsea Finn. Direct preference optimization: Your language model is secretly a reward model. *Advances in neural information processing systems*, 36:53728–53741, 2023.

Rouhollah Rahmatizadeh, Pooya Abolghasemi, Ladislau Bölöni, and Sergey Levine. Vision-based multi-task manipulation for inexpensive robots using end-to-end learning from demonstration. In *2018 IEEE international conference on robotics and automation (ICRA)*, pp. 3758–3765. IEEE, 2018.

Nived Rajaraman, Lin Yang, Jiantao Jiao, and Kannan Ramchandran. Toward the fundamental limits of imitation learning. *Advances in Neural Information Processing Systems*, 33:2914–2924, 2020.

Rajkumar Ramamurthy, Prithviraj Ammanabrolu, Kianté Brantley, Jack Hessel, Rafet Sifa, Christian Bauckhage, Hannaneh Hajishirzi, and Yejin Choi. Is reinforcement learning (not) for natural language processing: Benchmarks, baselines, and building blocks for natural language policy optimization. *arXiv preprint arXiv:2210.01241*, 2022.

Allen Z Ren, Justin Lidard, Lars L Ankile, Anthony Simeonov, Pulkit Agrawal, Anirudha Majumdar, Benjamin Burchfiel, Hongkai Dai, and Max Simchowitz. Diffusion policy policy optimization. *arXiv preprint arXiv:2409.00588*, 2024.

Corby Rosset, Ching-An Cheng, Arindam Mitra, Michael Santacroce, Ahmed Awadallah, and Tengyang Xie. Direct nash optimization: Teaching language models to self-improve with general preferences. *arXiv preprint arXiv:2404.03715*, 2024.

Daniel Russo. Worst-case regret bounds for exploration via randomized value functions. *Advances in neural information processing systems*, 32, 2019.

Daniel Russo and Benjamin Van Roy. Learning to optimize via posterior sampling. *Mathematics of Operations Research*, 39(4):1221–1243, 2014.

Daniel J Russo, Benjamin Van Roy, Abbas Kazerouni, Ian Osband, Zheng Wen, et al. A tutorial on thompson sampling. *Foundations and Trends® in Machine Learning*, 11(1):1–96, 2018.

Nur Muhammad Shafiullah, Zichen Cui, Ariuntuya Arty Altanzaya, and Lerrel Pinto. Behavior transformers: Cloning  $k$  modes with one stone. *Advances in neural information processing systems*, 35:22955–22968, 2022.

Zhihong Shao, Peiyi Wang, Qihao Zhu, Runxin Xu, Junxiao Song, Xiao Bi, Haowei Zhang, Mingchuan Zhang, YK Li, Yang Wu, et al. Deepseekmath: Pushing the limits of mathematical reasoning in open language models. *arXiv preprint arXiv:2402.03300*, 2024.

Pranav Shyam, Wojciech Jaśkowski, and Faustino Gomez. Model-based active exploration. In *International conference on machine learning*, pp. 5779–5788. PMLR, 2019.

Jascha Sohl-Dickstein, Eric Weiss, Niru Maheswaranathan, and Surya Ganguli. Deep unsupervised learning using nonequilibrium thermodynamics. In *International conference on machine learning*, pp. 2256–2265. pmlr, 2015.

Jiaming Song, Chenlin Meng, and Stefano Ermon. Denoising diffusion implicit models. *arXiv preprint arXiv:2010.02502*, 2020.

Jacob Mitchell Springer, Sachin Goyal, Kaiyue Wen, Tanishq Kumar, Xiang Yue, Sadhika Malladi, Graham Neubig, and Aditi Raghunathan. Overtrained language models are harder to fine-tune. *arXiv preprint arXiv:2503.19206*, 2025.

Ajay Sridhar, Dhruv Shah, Catherine Glossop, and Sergey Levine. Nomad: Goal masked diffusion policies for navigation and exploration. In *2024 IEEE International Conference on Robotics and Automation (ICRA)*, pp. 63–70. IEEE, 2024.

Bradly C Stadie, Sergey Levine, and Pieter Abbeel. Incentivizing exploration in reinforcement learning with deep predictive models. *arXiv preprint arXiv:1507.00814*, 2015.

Simon Stepputtis, Joseph Campbell, Mariano Phiellipp, Stefan Lee, Chitta Baral, and Heni Ben Amor. Language-conditioned imitation learning for robot manipulation tasks. *Advances in Neural Information Processing Systems*, 33:13139–13150, 2020.

Gokul Swamy, Christoph Dann, Rahul Kidambi, Zhiwei Steven Wu, and Alekh Agarwal. A minimaximalist approach to reinforcement learning from human feedback. *arXiv preprint arXiv:2401.04056*, 2024.

Yunhao Tang, Zhaohan Daniel Guo, Zeyu Zheng, Daniele Calandriello, Rémi Munos, Mark Rowland, Pierre Harvey Richemond, Michal Valko, Bernardo Ávila Pires, and Bilal Piot. Generalized preference optimization: A unified approach to offline alignment. *arXiv preprint arXiv:2402.05749*, 2024.

Voot Tangkaratt, Nontawat Charoenphakdee, and Masashi Sugiyama. Robust imitation learning from noisy demonstrations. *arXiv preprint arXiv:2010.10181*, 2020.

Kimi Team, Angang Du, Bofei Gao, Bowei Xing, Changjiu Jiang, Cheng Chen, Cheng Li, Chenjun Xiao, Chenzhuang Du, Chonghua Liao, et al. Kimi k1. 5: Scaling reinforcement learning with llms. *arXiv preprint arXiv:2501.12599*, 2025.

Octo Model Team, Dibya Ghosh, Homer Walke, Karl Pertsch, Kevin Black, Oier Mees, Sudeep Dasari, Joey Hejna, Tobias Kreiman, Charles Xu, et al. Octo: An open-source generalist robot policy. *arXiv preprint arXiv:2405.12213*, 2024.

William R Thompson. On the likelihood that one unknown probability exceeds another in view of the evidence of two samples. *Biometrika*, 25(3/4):285–294, 1933.

Hugo Touvron, Louis Martin, Kevin Stone, Peter Albert, Amjad Almahairi, Yasmine Babaei, Nikolay Bashlykov, Soumya Batra, Prajjwal Bhargava, Shruti Bhosale, et al. Llama 2: Open foundation and fine-tuned chat models. *arXiv preprint arXiv:2307.09288*, 2023.

Ikechukwu Uchendu, Ted Xiao, Yao Lu, Banghua Zhu, Mengyuan Yan, Joséphine Simon, Matthew Bennice, Chuyuan Fu, Cong Ma, Jiantao Jiao, et al. Jump-start reinforcement learning. In *International Conference on Machine Learning*, pp. 34556–34583. PMLR, 2023.

Andrew Wagenmaker, Mitsuhiko Nakamoto, Yunchu Zhang, Seohong Park, Waleed Yagoub, Anusha Nagabandi, Abhishek Gupta, and Sergey Levine. Steering your diffusion policy with latent space reinforcement learning. *arXiv preprint arXiv:2506.15799*, 2025a.

Andrew Wagenmaker, Zhiyuan Zhou, and Sergey Levine. Behavioral exploration: Learning to explore via in-context adaptation. In *Forty-second International Conference on Machine Learning*, 2025b.

Homer Rich Walke, Kevin Black, Tony Z Zhao, Quan Vuong, Chongyi Zheng, Philippe Hansen-Estruch, Andre Wang He, Vivek Myers, Moo Jin Kim, Max Du, et al. Bridgedata v2: A dataset for robot learning at scale. In *Conference on Robot Learning*, pp. 1723–1736. PMLR, 2023.

Jane X Wang, Zeb Kurth-Nelson, Dhruva Tirumala, Hubert Soyer, Joel Z Leibo, Remi Munos, Charles Blundell, Dharshan Kumaran, and Matt Botvinick. Learning to reinforcement learn. *arXiv preprint arXiv:1611.05763*, 2016.

Yunke Wang, Chang Xu, and Bo Du. Robust adversarial imitation learning via adaptively-selected demonstrations. In *IJCAI*, pp. 3155–3161, 2021.

Max Wilcoxson, Qiyang Li, Kevin Frans, and Sergey Levine. Leveraging skills from unlabeled prior data for efficient online exploration. *arXiv preprint arXiv:2410.18076*, 2024.

Charles Xu, Qiyang Li, Jianlan Luo, and Sergey Levine. Rldg: Robotic generalist policy distillation via reinforcement learning. *arXiv preprint arXiv:2412.09858*, 2024.

Haoran Xu, Xianyuan Zhan, Honglei Yin, and Hailing Qin. Discriminator-weighted offline imitation learning from suboptimal demonstrations. In *International Conference on Machine Learning*, pp. 24725–24742. PMLR, 2022.

Yueqin Yin, Zhendong Wang, Yi Gu, Hai Huang, Weizhu Chen, and Mingyuan Zhou. Relative preference optimization: Enhancing llm alignment through contrasting responses across identical and diverse prompts. *arXiv preprint arXiv:2402.10958*, 2024.

Xiu Yuan, Tongzhou Mu, Stone Tao, Yunhao Fang, Mengke Zhang, and Hao Su. Policy decorator: Model-agnostic online refinement for large policy model. *arXiv preprint arXiv:2412.13630*, 2024.

Sheng Yue, Xingyuan Hua, Ju Ren, Sen Lin, Junshan Zhang, and Yaoxue Zhang. Ollie: Imitation learning from offline pretraining to online finetuning. *arXiv preprint arXiv:2405.17477*, 2024.

Yang Yue, Zhiqi Chen, Rui Lu, Andrew Zhao, Zhaokai Wang, Shiji Song, and Gao Huang. Does reinforcement learning really incentivize reasoning capacity in llms beyond the base model? *arXiv preprint arXiv:2504.13837*, 2025.

Yanjie Ze, Gu Zhang, Kangning Zhang, Chenyuan Hu, Muhan Wang, and Huazhe Xu. 3d diffusion policy: Generalizable visuomotor policy learning via simple 3d representations. *arXiv preprint arXiv:2403.03954*, 2024.

Hansi Zeng, Kai Hui, Honglei Zhuang, Zhen Qin, Zhenrui Yue, Hamed Zamani, and Dana Alon. Can pre-training indicators reliably predict fine-tuning outcomes of llms? *arXiv preprint arXiv:2504.12491*, 2025.

Haichao Zhang, We Xu, and Haonan Yu. Policy expansion for bridging offline-to-online reinforcement learning. *arXiv preprint arXiv:2302.00935*, 2023.

Tianhao Zhang, Zoe McCarthy, Owen Jow, Dennis Lee, Xi Chen, Ken Goldberg, and Pieter Abbeel. Deep imitation learning for complex manipulation tasks from virtual reality teleoperation. In *2018 IEEE international conference on robotics and automation (ICRA)*, pp. 5628–5635. IEEE, 2018.

Zijian Zhang, Kaiyuan Zheng, Zhaorun Chen, Joel Jang, Yi Li, Siwei Han, Chaoqi Wang, Mingyu Ding, Dieter Fox, and Huaxiu Yao. Grape: Generalizing robot policy via preference alignment. *arXiv preprint arXiv:2411.19309*, 2024.

Tony Z Zhao, Jonathan Tompson, Danny Driess, Pete Florence, Kamyar Ghasemipour, Chelsea Finn, and Ayzaan Wahid. Aloha unleashed: A simple recipe for robot dexterity. *arXiv preprint arXiv:2410.13126*, 2024.

Han Zheng, Xufang Luo, Pengfei Wei, Xuan Song, Dongsheng Li, and Jing Jiang. Adaptive policy learning for offline-to-online reinforcement learning. In *Proceedings of the AAAI Conference on Artificial Intelligence*, volume 37, pp. 11372–11380, 2023.

Brian D Ziebart, Andrew L Maas, J Andrew Bagnell, Anind K Dey, et al. Maximum entropy inverse reinforcement learning. In *Aaai*, volume 8, pp. 1433–1438. Chicago, IL, USA, 2008.

Daniel M Ziegler, Nisan Stiennon, Jeffrey Wu, Tom B Brown, Alec Radford, Dario Amodei, Paul Christiano, and Geoffrey Irving. Fine-tuning language models from human preferences. *arXiv preprint arXiv:1909.08593*, 2019.

Luisa Zintgraf, Kyriacos Shiarlis, Maximilian Igl, Sebastian Schulze, Yarin Gal, Katja Hofmann, and Shimon Whiteson. Varibad: A very good method for bayes-adaptive deep rl via meta-learning. *arXiv preprint arXiv:1910.08348*, 2019.

## A Additional Related Work

**Other approaches for pretraining from demonstrations.** While our primary focus is on behavioral cloning (as noted, the workhorse of most modern applications) other approaches to pretraining from demonstrations exist. BC is only one possible instantiation of *imitation learning*; other approaches to imitation learning include inverse RL (Ng et al., 2000; Abbeel & Ng, 2004; Ziebart et al., 2008), methods that aim to learn a policy matching the state distribution of the demonstrator, such as adversarial imitation learning (Ho & Ermon, 2016; Kostrikov et al., 2018; Fu et al., 2017; Kostrikov et al., 2019; Ni et al., 2021; Garg et al., 2021; Xu et al., 2022; Li et al., 2023b; Yue et al., 2024), and robust imitation learning (Chae et al., 2022; Desai et al., 2020; Tangkaratt et al., 2020; Wang et al., 2021; Giannarino et al., 2025). The majority of these works, however, either assume access to additional data sources (e.g. suboptimal trajectories), or require online environment access and are therefore not truly offline pretraining approaches, which is the focus of this work. Furthermore, none of these works explicitly consider the role of pretraining in enabling efficient RL finetuning.

Meta-learning directly aims learn an initialization that can be quickly adapted to a new task. While instantiations of meta-learning for imitation learning exist (Duan et al., 2017; Finn et al., 2017b; James et al., 2018; Dasari & Gupta, 2021; Gao et al., 2023), our setting differs fundamentally from the meta-imitation learning setting. Meta-imitation learning assumes access to demonstration data from *more than one task*, and attempts to learn an initialization that will allow for quickly adapting to demonstrations from a *new task*. In contrast, our goal is to obtain an approach able to learn on a *single task* (though we also consider the multi-task setting), and we aim to find an initialization that allows for improvement on the *same task*, while preserving pretrained performance on this task. Furthermore, rather than learning from new *demonstrations*, as meta-imitation learning does, we aim to learn from (potentially suboptimal) data collected online and that is labeled with rewards.

**Reinforcement learning-based pretraining.** In the RL literature, two lines of work bear some resemblance to ours as well. The *offline-to-online RL* setting aims to train policies with RL on offline datasets that can then be improved with further online interaction (Lee et al., 2022; Ghosh et al., 2022; Kumar et al., 2022; Zhang et al., 2023; Uchendu et al., 2023; Zheng et al., 2023; Ball et al., 2023; Nakamoto et al., 2023), and the *meta-RL* setting aims to meta-learn a policy on some set of tasks which can then be quickly adapted to a new task (Wang et al., 2016; Duan et al., 2016; Finn et al., 2017a, 2018). While similar to our work in that these works also aim to learn behaviors that can be efficiently improved online, the settings differ significantly in that the offline- or meta-pretraining typically requires reward labels (rather than unlabeled demonstrations) and are performed with RL (rather than BC)—in contrast, we study how BC-like pretraining (as noted, the workhorse of most modern applications) can enable efficient online adaptation.

## B Proofs

### B.1 BC Policy Fails to Cover Demonstrator Actions

*Proof of Proposition 2.* Let  $\mathcal{M}^1$  and  $\mathcal{M}^2$  denote multi-armed bandits with 3 arms and reward functions  $r^1$  and  $r^2$ :

$$\begin{aligned} r^1(a_1) &= 0, r^1(a_2) = 1, r^1(a_3) = 0 \\ r^2(a_1) &= 0, r^2(a_2) = 0, r^2(a_3) = 1. \end{aligned}$$

Let  $\pi^\beta(a_1) = 1 - 4\epsilon$ ,  $\pi^\beta(a_2) = 2\epsilon$ ,  $\pi^\beta(a_3) = 2\epsilon$ .

By construction of  $\hat{\pi}^{\text{bc}}$ , if  $T(a_2) = 0$  then we will have  $\hat{\pi}^{\text{bc}}(a_2) = 0$ , and if  $T(a_3) = 0$  we will have  $\hat{\pi}^{\text{bc}}(a_3) = 0$ . By the definition of both  $\mathcal{M}^1$  and  $\mathcal{M}^2$ , we have

$$\mathbb{P}^{\mathcal{M}^i}[T(a_2) = 0, T(a_3) = 0] = (1 - 4\epsilon)^T.$$

As we have assumed that  $T \leq \frac{1}{20\epsilon}$  and  $\epsilon \in (0, 1/8]$ , some calculation shows that we can lower bound this as  $1/2$ . Note that for both  $\mathcal{M}^1$  and  $\mathcal{M}^2$ , we have  $\mathcal{J}(\pi^\beta) = 2\epsilon$ , while for policies  $\hat{\pi}^{\text{bc}}$  that only play  $a_1$ , we have  $\mathcal{J}(\hat{\pi}^{\text{bc}}) = 0$ . This proves the first part of the result.

For the second part, note that the optimal policy on  $\mathcal{M}^1$  plays only  $a_2$  and has expected reward of 1, while the optimal policy on  $\mathcal{M}^2$  plays only  $a_2$  and has expected reward of 1. Let  $\hat{\pi}$  denote an

estimate of the optimal policy and  $\mathbb{E}^{\mathcal{M}^i, \hat{\pi}^{\text{bc}}}[\cdot]$  the expectation induced by playing the policy  $\hat{\pi}^{\text{bc}}$  from the first part on instance  $\mathcal{M}^i$ . Then:

$$\min_{\hat{\pi}} \max_{i \in \{1, 2\}} \mathbb{E}^{\mathcal{M}^i, \hat{\pi}^{\text{bc}}} \left[ \max_{\pi} \mathcal{J}^{\mathcal{M}^i}(\pi) - \mathcal{J}^{\mathcal{M}^i}(\hat{\pi}) \right] = \min_{\hat{\pi}} \max_{i \in \{1, 2\}} \mathbb{E}^{\mathcal{M}^i, \hat{\pi}^{\text{bc}}} [1 - \hat{\pi}(a_{1+i})].$$

Note that  $1 - \hat{\pi}(a_2) = \hat{\pi}(a_1) + \hat{\pi}(a_3) \geq \hat{\pi}(a_3)$ . Thus we can lower bound the above as

$$\begin{aligned} & \geq \min_{\hat{\pi}} \max \{ \mathbb{E}^{\mathcal{M}^1, \hat{\pi}^{\text{bc}}}[\hat{\pi}(a_3)], \mathbb{E}^{\mathcal{M}^2, \hat{\pi}^{\text{bc}}}[1 - \hat{\pi}(a_3)] \} \\ & \geq \min_{\hat{\pi}} \frac{1}{2} \left( \mathbb{E}^{\mathcal{M}^1, \hat{\pi}^{\text{bc}}}[\hat{\pi}(a_3)] + \mathbb{E}^{\mathcal{M}^2, \hat{\pi}^{\text{bc}}}[1 - \hat{\pi}(a_3)] \right) \\ & \geq \frac{1}{2} - \frac{1}{2} \min_{\hat{\pi}} \left| \mathbb{E}^{\mathcal{M}^1, \hat{\pi}^{\text{bc}}}[\hat{\pi}(a_3)] - \mathbb{E}^{\mathcal{M}^2, \hat{\pi}^{\text{bc}}}[\hat{\pi}(a_3)] \right|. \end{aligned}$$

We can bound

$$\left| \mathbb{E}^{\mathcal{M}^1, \hat{\pi}^{\text{bc}}}[\hat{\pi}(a_3)] - \mathbb{E}^{\mathcal{M}^2, \hat{\pi}^{\text{bc}}}[\hat{\pi}(a_3)] \right| \leq \text{TV}(\mathbb{P}^{\mathcal{M}^1, \hat{\pi}^{\text{bc}}}, \mathbb{P}^{\mathcal{M}^2, \hat{\pi}^{\text{bc}}}).$$

Since  $\mathcal{M}^1$  and  $\mathcal{M}^2$  only differ on  $a_2$  and  $a_3$ , and since  $\hat{\pi}^{\text{bc}}(a_2) = \hat{\pi}^{\text{bc}}(a_3) = 0$ , we have  $\text{TV}(\mathbb{P}^{\mathcal{M}^1, \hat{\pi}^{\text{bc}}}, \mathbb{P}^{\mathcal{M}^2, \hat{\pi}^{\text{bc}}}) = 0$ . Thus, we conclude that

$$\min_{\hat{\pi}} \max_{i \in \{1, 2\}} \mathbb{E}^{\mathcal{M}^i, \hat{\pi}^{\text{bc}}} \left[ \max_{\pi} \mathcal{J}^{\mathcal{M}^i}(\pi) - \mathcal{J}^{\mathcal{M}^i}(\hat{\pi}) \right] \geq \frac{1}{2}.$$

This proves the second part of the result.  $\square$

## B.2 Uniform Noise Fails

*Proof of Proposition 3. Construction.* Let  $\mathcal{M}$  be the MDP with state space  $\{\tilde{s}_1, \dots, \tilde{s}_k, s_1, s_2\}$ , actions  $\{a_1, a_2\}$ , horizon  $H \geq 2$  with initial state distribution:

$$P_0(s_1) = 1/2, \quad P_0(\tilde{s}_1) = 2^{-2} + 2^{-k}, \quad P_0(\tilde{s}_i) = 2^{-i-1}, i \geq 2,$$

transition function, for all  $h \in [H]$ :

$$\begin{aligned} P_h(\tilde{s}_i \mid \tilde{s}_i, a) &= 1, \forall a \in \mathcal{A}, \quad P_h(s_1 \mid s_1, a_1) = 1, \\ P_h(s_2 \mid s_1, a_2) &= 1, \quad P_h(s_2 \mid s_2, a) = 1, \forall a \in \mathcal{A}, \end{aligned}$$

and reward that is 0 everywhere except

$$r_1(\tilde{s}_i, a_1) = r_H(s_1, a_1) = 1, \quad r_1(\tilde{s}_i, a_2) = 1 - 2\Delta,$$

for some  $\Delta > 0$  to be specified. We consider  $\pi^\beta$  defined as

$$\pi_h^\beta(a_1 \mid \tilde{s}_i) = \pi_h^\beta(a_2 \mid \tilde{s}_i) = \frac{1}{2}, \quad \pi_h^\beta(a_1 \mid s_1) = 1.$$

Let  $\epsilon := \frac{H^2 S \log T}{T} + \xi$ , and set  $\Delta \leftarrow 2\epsilon$ .

**Upper bound on  $\alpha$ .** Note that  $\mathcal{J}(\pi^\beta) = 1 - \frac{1}{2}\Delta$ , and that the value of the optimal policy  $\pi^*$  is  $\mathcal{J}(\pi^*) = \max_{\pi} \mathcal{J}(\pi) = 1$ . Let  $\tilde{\pi}^{\text{u}, \alpha}$  denote the policy that, on all  $\tilde{s}_i$  plays  $\pi^*$ , and on other states plays  $\pi^*$  with probability  $1 - \alpha$ , and otherwise plays  $\text{unif}(\mathcal{A})$ . Note then that, regardless of the value of  $\hat{\pi}^{\text{bc}}$ , we have that  $\mathcal{J}(\tilde{\pi}^{\text{u}, \alpha}) \geq \mathcal{J}(\hat{\pi}^{\text{u}, \alpha})$ . Thus,

$$\mathcal{J}(\pi^\beta) - \mathbb{E}[\mathcal{J}(\hat{\pi}^{\text{u}, \alpha})] \geq \mathcal{J}(\pi^\beta) - \mathcal{J}(\tilde{\pi}^{\text{u}, \alpha})$$

If we are in  $s_1$  at  $h = 2$ , the only way we can receive any reward on the episode is if we take action  $a_1$  for the last  $H - 1$  steps, and we then receive a reward of 1. Under  $\tilde{\pi}^{\text{u}, \alpha}$ , we take  $a_1$  at each step with probability  $1 - \alpha + \alpha/A$ , so our probability of getting a reward of 1 is  $(1 - \alpha + \alpha/A)^{H-1}$ . Note that in contrast  $\pi^\beta$  will always play  $a_1$  and receive a reward of 1 in this situation. If we are in  $\tilde{s}_i$  at  $h = 2$  for any  $i$ , then  $\pi^\beta$  will incur a loss of  $\Delta$  more than  $\tilde{\pi}^{\text{u}, \alpha}$ . Thus, we can lower bound

$$\mathcal{J}(\pi^\beta) - \mathcal{J}(\tilde{\pi}^{\text{u}, \alpha}) \geq -\frac{1}{2}\Delta + \frac{1}{2} \cdot (1 - (1 - \alpha + \alpha/A)^{H-1})$$

By assumption we have that  $\frac{1}{2}\Delta = \epsilon$ . Thus, if we want  $\mathcal{J}(\pi^\beta) - \mathbb{E}[\mathcal{J}(\hat{\pi}^{u,\alpha})] \leq \epsilon$ , we need

$$\frac{1}{2} \cdot (1 - (1 - \alpha + \alpha/A)^{H-1}) \leq 2\epsilon.$$

Rearranging this, we have

$$1 - 4\epsilon \leq (1 - \alpha + \alpha/A)^{H-1} \iff \frac{1}{H-1} \log(1 - 4\epsilon) \leq \log(1 - \alpha + \alpha/A).$$

From the Taylor decomposition of  $\log(1 - x)$ , we see that  $\log(1 - \alpha + \alpha/A) \leq -(1 - 1/A)\alpha$ . Furthermore, we can lower bound

$$\log(1 - 4\epsilon) \geq -8\epsilon$$

as long as  $\epsilon \leq 1/2$ . Altogether, then, we have

$$\frac{-8\epsilon}{H-1} \leq -(1 - 1/A)\alpha \implies \alpha \leq \frac{8\epsilon}{(H-1)(1 - 1/A)} \implies \alpha \leq 32\epsilon$$

where the last inequality follows since  $H \geq 2, A = 2$ .

**Upper bound on  $\gamma$ .** Let  $i_T := \arg \max_i \{2^{-i-1} \mid 2^{-i-1} \leq 1/T\}$ , so that  $1/2T \leq P_0(\tilde{s}_{i_T}) \leq 1/T$ , and note that such an  $\tilde{s}_{i_T}$  exists by construction. Let  $\mathcal{E}$  be the event  $\mathcal{E} := \{T_1(\tilde{s}_{i_T}) = T_1(\tilde{s}_{i_T}, a_2) = 1\}$ . We have

$$\begin{aligned} \mathbb{P}[\mathcal{E}] &= \mathbb{P}[T_1(\tilde{s}_{i_T}, a_2) = 1 \mid T_1(\tilde{s}_{i_T}) = 1] \mathbb{P}[T_1(\tilde{s}_{i_T}) = 1] \\ &= \frac{1}{2} \cdot T P_0(\tilde{s}_{i_T}) (1 - P_0(\tilde{s}_{i_T}))^{T-1} \\ &= \frac{1}{2} \cdot T \cdot \frac{1}{2T} \cdot (1 - \frac{1}{T})^{T-1} \\ &\geq \frac{1}{4e}. \end{aligned}$$

Note that on the event  $\mathcal{E}$ , we have  $\hat{\pi}_1^{\text{bc}}(a_1 \mid \tilde{s}_{i_T}) = 0$ , but  $\pi_1^\beta(a_1 \mid \tilde{s}_{i_T}) = 1/2$ . Thus,

$$\hat{\pi}_1^{u,\alpha}(a_1 \mid \tilde{s}_{i_T}) = \alpha/A \leq 32\epsilon/A = 64\epsilon/A \cdot \pi_1^\beta(a_1 \mid \tilde{s}_{i_T})$$

where we have used the bound on  $\alpha$  shown above. Thus, on  $\mathcal{E}$ , we will only have that  $\hat{\pi}^{u,\alpha}$  achieves demonstrator action coverage for  $\gamma \leq 64\epsilon/A$ . Since  $\mathcal{E}$  occurs with probability at least  $1/4e$ , it follows that if we want to guarantee  $\hat{\pi}^{u,\alpha}$  achieves demonstrator action coverage with probability at least  $1 - \delta$  for  $\delta < 1/4e$ , we must have  $\gamma \leq 64\epsilon/A$ .

Note as well that, since  $\hat{\pi}_1^{\text{bc}}(a_2 \mid \tilde{s}_{i_T}) = 1$ , any policy in the support of  $\hat{\pi}^{\text{bc}}$  will be suboptimal by a factor of at least  $P_0(\tilde{s}_{i_T}) \cdot 2\Delta \geq \Delta/T$ .  $\square$

### B.3 Analysis of Posterior Demonstrator Policy

Throughout this section we denote

$$\tilde{\pi}_h(a \mid s) := \begin{cases} (1 - \alpha) \cdot \frac{T_h(s,a)}{T_h(s)} + \alpha \cdot \frac{T_h(s,a) + \lambda/A}{T_h(s) + \lambda} & T_h(s) > 0 \\ \text{unif}(\mathcal{A}) & T_h(s) = 0 \end{cases}$$

for some  $\alpha \in [0, 1]$ .

We also denote  $w_h^\pi(s, a) := \mathbb{P}^\pi[s_h = s, a_h = a]$ .  $Q_h^\pi(s, a) := \mathbb{E}^\pi[\sum_{h' \geq h} r_{h'}(s_{h'}, a_{h'}) \mid s_h = s, a_h = a]$  denotes the standard  $Q$ -function.  $\mathcal{J}(\pi; r)$  denotes the expected return of policy  $\pi$  for reward  $r$ .

**Lemma 1.** *As long as  $\delta \leq 0.9$  and  $\lambda \geq A$ , we have*

$$\mathbb{P}\left[\tilde{\pi}_h(a \mid s) \geq \alpha \cdot \min\left\{\frac{\pi_h^\beta(a \mid s)}{64 \log SH/\delta}, \frac{1}{2\lambda}\right\}, \forall a \in \mathcal{A}, s \in \mathcal{S}, h \in [H]\right] \geq 1 - \delta.$$

*Proof.* Consider some  $(s, h)$ . By Bernstein's inequality, if  $T_h(s) > 0$ , we have that with probability at least  $1 - \delta$ ,

$$\frac{T_h(s, a)}{T_h(s)} \geq \pi_h^\beta(a | s) - \sqrt{\frac{2\pi_h^\beta(a | s) \log 1/\delta}{T_h(s)}} - \frac{2 \log 1/\delta}{3T_h(s)}. \quad (3)$$

From some algebra, we see that as long as  $T_h(s) \geq \frac{32 \log 1/\delta}{\pi_h^\beta(a | s)}$ , we have that  $\frac{T_h(s, a)}{T_h(s)} \geq \frac{1}{2} \pi_h^\beta(a | s)$ . By the definition of  $\tilde{\pi}$ , under the good event of (3) we can then lower bound

$$\begin{aligned} \tilde{\pi}_h(a | s) &\geq \begin{cases} \frac{\alpha}{1 + \lambda/T_h(s)} \cdot \frac{1}{2} \pi_h^\beta(a | s) & T_h(s) \geq \frac{32 \log 1/\delta}{\pi_h^\beta(a | s)} \\ \frac{\alpha \lambda / A}{T_h(s) + A} & \text{o.w.} \end{cases} \\ &\geq \begin{cases} \frac{\alpha \cdot 32 \log 1/\delta}{32 \log 1/\delta + \lambda \cdot \pi_h^\beta(a | s)} \cdot \frac{1}{2} \pi_h^\beta(a | s) & N_h(s) \geq \frac{32 \log 1/\delta}{\pi_h^\beta(a | s)} \\ \frac{\alpha \lambda / A \cdot \pi_h^\beta(a | s)}{32 \log 1/\delta + \lambda \cdot \pi_h^\beta(a | s)} & \text{o.w.} \end{cases} \\ &\stackrel{(a)}{\geq} \frac{\alpha \cdot \pi_h^\beta(a | s)}{32 \log 1/\delta + \lambda \cdot \pi_h^\beta(a | s)} \\ &\geq \alpha \cdot \min \left\{ \frac{\pi_h^\beta(a | s)}{64 \log 1/\delta}, \frac{1}{2\lambda} \right\} \end{aligned}$$

where (a) follows as long as  $\delta \leq 0.9$  and  $\lambda \geq A$ . In the case when  $T_h(s) = 0$  we have  $\tilde{\pi}_h(a | s) = 1/A \geq 1/\lambda$ , so this lower bound still holds. Taking a union bound over arms proves the result.  $\square$

**Lemma 2.** *As long as  $\lambda \geq 4 \log(HT)$ , we have*

$$\mathbb{E}[\mathcal{J}(\hat{\pi}^{\text{bc}}) - \mathcal{J}(\tilde{\pi})] \lesssim (1 + \alpha H) \cdot \frac{H^2 S \log T}{T} + \alpha \cdot \frac{H^2 S \lambda}{T}.$$

*Proof.* By the Performance-Difference Lemma we have:

$$\begin{aligned} \mathcal{J}(\hat{\pi}^{\text{bc}}) - \mathcal{J}(\tilde{\pi}) &= \sum_{h=1}^H \sum_{s \in \mathcal{S}} w_h^{\hat{\pi}^{\text{bc}}}(s) \cdot \left( \mathbb{E}_{a \sim \hat{\pi}_h^{\text{bc}}(s)}[Q_h^{\tilde{\pi}}(s, a)] - \mathbb{E}_{a \sim \tilde{\pi}_h(s)}[Q_h^{\tilde{\pi}}(s, a)] \right) \\ &\leq \sum_{h=1}^H \sum_{s \in \mathcal{S}} w_h^{\hat{\pi}^{\text{bc}}}(s) \cdot \left| \mathbb{E}_{a \sim \hat{\pi}_h^{\text{bc}}(s)}[Q_h^{\tilde{\pi}}(s, a)] - \mathbb{E}_{a \sim \tilde{\pi}_h(s)}[Q_h^{\tilde{\pi}}(s, a)] \right|. \end{aligned} \quad (4)$$

For  $(s, h)$  with  $N_h(s) > 0$ , we have

$$\left| \mathbb{E}_{a \sim \hat{\pi}_h^{\text{bc}}(s)}[Q_h^{\tilde{\pi}}(s, a)] - \mathbb{E}_{a \sim \tilde{\pi}_h(s)}[Q_h^{\tilde{\pi}}(s, a)] \right| \leq \sum_{a \in \mathcal{A}} H \cdot |\hat{\pi}_h^{\text{bc}}(a | s) - \tilde{\pi}_h(a | s)|,$$

where we have used that  $Q_h^{\hat{\pi}^{\text{post}}}(s, a) \in [0, H]$ . Then, using the definition of  $\hat{\pi}^{\text{bc}}$  and  $\tilde{\pi}$  we can bound this as

$$\begin{aligned} &\leq \sum_{a \in \mathcal{A}} \alpha H \cdot \left| \frac{T_h(s, a)}{T_h(s)} - \frac{T_h(s, a) + \lambda/A}{T_h(s) + \lambda} \right| \\ &= \sum_{a \in \mathcal{A}} \frac{\alpha \lambda H}{A} \cdot \left| \frac{AT_h(s, a) - T_h(s)}{T_h(s)(T_h(s) + \lambda)} \right| \\ &\leq \sum_{a \in \mathcal{A}} \frac{\alpha \lambda H}{A} \cdot \frac{AT_h(s, a) + T_h(s)}{T_h(s)(T_h(s) + \lambda)} \\ &= \frac{2\alpha \lambda H}{T_h(s) + \lambda}. \end{aligned}$$

Since  $\mathbb{E}_{a \sim \hat{\pi}_h^{\text{bc}}(s)}[Q_h^{\tilde{\pi}}(s, a)] - \mathbb{E}_{a \sim \tilde{\pi}_h(s)}[Q_h^{\tilde{\pi}}(s, a)] = 0$  by construction when  $T_h(s) = 0$ , we then have

$$(4) \leq \sum_{h=1}^H \sum_{s \in \mathcal{S}} w_h^{\hat{\pi}^{\text{bc}}}(s) \cdot \frac{2\alpha \lambda H}{T_h(s) + \lambda}.$$

Let  $\mathcal{E}$  denote the good event from Lemma 3 with  $\delta = \frac{S}{T}$ . Then as long as  $\lambda \geq 4 \log(HT)$  we can bound the above as

$$\begin{aligned} &\leq \sum_{h=1}^H \sum_{s \in \mathcal{S}} w_h^{\hat{\pi}^{\text{bc}}}(s) \cdot \frac{2\alpha\lambda H}{T_h(s) + \lambda} \mathbb{I}\{\mathcal{E}\} + 2H^2 \cdot \mathbb{I}\{\mathcal{E}^c\} \\ &\leq \sum_{h=1}^H \sum_{s \in \mathcal{S}} w_h^{\hat{\pi}^{\text{bc}}}(s) \cdot \frac{4\alpha\lambda H}{w_h^{\pi^\beta}(s) \cdot T + \lambda} + 2H^2 \cdot \mathbb{I}\{\mathcal{E}^c\}. \end{aligned}$$

Let  $\tilde{r}$  denote the reward function:

$$\tilde{r}_h(s, a) := \frac{\lambda}{w_h^{\pi^\beta}(s) \cdot T + \lambda}$$

and note that  $\tilde{r} \in [0, 1]$ , and

$$\sum_{h=1}^H \sum_{s \in \mathcal{S}} w_h^{\hat{\pi}^{\text{bc}}}(s) \cdot \frac{4\alpha\lambda H}{w_h^{\pi^\beta}(s) \cdot T + \lambda} = 4\alpha H \cdot \mathcal{J}(\hat{\pi}^{\text{bc}}; \tilde{r}).$$

By Theorem 4.4 of Rajaraman et al. (2020), we have<sup>2</sup>

$$\begin{aligned} \mathbb{E}[\mathcal{J}(\hat{\pi}^{\text{bc}}; \tilde{r})] &\lesssim \mathcal{J}(\pi^\beta; \tilde{r}) + \frac{H^2 S \log T}{T} \\ &= \sum_{h=1}^H \sum_{s \in \mathcal{S}} w_h^{\pi^\beta}(s) \cdot \frac{\lambda}{w_h^{\pi^\beta}(s) \cdot T + \lambda} + \frac{H^2 S \log T}{T} \\ &\leq \frac{HS\lambda}{T} + \frac{H^2 S \log T}{T}. \end{aligned}$$

Noting that  $\mathbb{E}[2H^2 \cdot \mathbb{I}\{\mathcal{E}^c\}] \leq 2H^2\delta \leq \frac{2H^2S}{T}$  completes the proof.  $\square$

**Lemma 3.** *With probability at least  $1 - \delta$ , for all  $(s, h)$ , we have*

$$T_h(s) + \lambda \geq \frac{1}{2} w_h^{\pi^\beta}(s) \cdot T + \frac{1}{2} \lambda$$

as long as  $\lambda \geq 4 \log \frac{SH}{\delta}$ .

*Proof.* Consider some  $(s, h)$  and note that  $\mathbb{E}[T_h(s)/T] = w_h^{\pi^\beta}(s)$ . By Bernstein's inequality, we have with probability  $1 - \delta/SH$ :

$$T_h(s) \geq w_h^{\pi^\beta}(s) \cdot T - \sqrt{2w_h^{\pi^\beta}(s) \cdot T \cdot \log \frac{SH}{\delta}} - \frac{2}{3} \log \frac{SH}{\delta}.$$

We would then like to show that

$$\begin{aligned} &w_h^{\pi^\beta}(s) \cdot T - \sqrt{2w_h^{\pi^\beta}(s) \cdot T \cdot \log \frac{SH}{\delta}} - \frac{2}{3} \log \frac{SH}{\delta} + \lambda \geq \frac{1}{2} (w_h^{\pi^\beta}(s) \cdot T + \lambda) \\ \iff &\frac{1}{2} w_h^{\pi^\beta}(s) \cdot T + \frac{1}{2} \lambda \geq \sqrt{2w_h^{\pi^\beta}(s) \cdot T \cdot \log \frac{SH}{\delta}} + \frac{2}{3} \log \frac{SH}{\delta} \end{aligned}$$

As we have assumed  $\lambda \geq 4 \log \frac{SH}{\delta}$ , it suffices to show

$$\frac{1}{2} w_h^{\pi^\beta}(s) \cdot T + \log \frac{SH}{\delta} \geq \sqrt{2w_h^{\pi^\beta}(s) \cdot T \cdot \log \frac{SH}{\delta}}.$$

However, this is true by the AM-GM inequality. A union bound proves the result.  $\square$

<sup>2</sup>Note that Theorem 4.4 of Rajaraman et al. (2020) shows an inequality in the opposite direction of what we show here: they bound  $\mathcal{J}(\pi^\beta; \tilde{r}) - \mathbb{E}[\mathcal{J}(\hat{\pi}^{\text{bc}}; \tilde{r})]$  instead of  $\mathbb{E}[\mathcal{J}(\hat{\pi}^{\text{bc}}; \tilde{r})] - \mathcal{J}(\pi^\beta; \tilde{r})$ . However, we see that the only place in their proof where their argument relied on this ordering is in Lemma A.8. We show in Lemma 4 that a reverse version of their Lemma A.8 holds, allowing us to instead bound  $\mathbb{E}[\mathcal{J}(\hat{\pi}^{\text{bc}}; \tilde{r})] - \mathcal{J}(\pi^\beta; \tilde{r})$ .

**Lemma 4** (Reversed version of Lemma A.8 of Rajaraman et al. (2020)). *Adopting the notation from Rajaraman et al. (2020), we have*

$$\mathbb{E}[\Pr_{\pi^{\text{first}}}[\mathcal{E}]] \leq \frac{SH \log N}{N}$$

for  $\mathcal{E}^c$  the event that within a trajectory, the policy only visits states for which  $T_h(s) > 0$ .

*Proof.* Let  $\mathcal{E}_{s,h}$  denote the event that the state  $s$  is visited at step  $h$  and  $T_h(s) = 0$ , and  $\mathcal{E}_h := \bigcup_{s \in \mathcal{S}} \mathcal{E}_{s,h}$ . Then, by simple set inclusions, we have:

$$\mathcal{E} = \bigcup_{h \in [H]} \bigcup_{s \in \mathcal{S}} \mathcal{E}_{s,h} = \bigcup_{h \in [H]} \bigcup_{s \in \mathcal{S}} \left( \mathcal{E}_{s,h} \cap \bigcap_{h' < h} \mathcal{E}_{h'}^c \right).$$

By a union bound it follows that

$$\mathbb{E}[\Pr_{\pi^{\text{first}}}[\mathcal{E}]] \leq \sum_{h \in [H]} \sum_{s \in \mathcal{S}} \mathbb{E}[\Pr_{\pi^{\text{first}}}[\mathcal{E}_{s,h} \cap \bigcap_{h' < h} \mathcal{E}_{h'}^c]].$$

Now note that

$$\begin{aligned} \Pr_{\pi^{\text{first}}}[\mathcal{E}_{s,h} \cap \bigcap_{h' < h} \mathcal{E}_{h'}^c] &= \Pr_{\pi^{\text{first}}}[\mathcal{E}_{s,h} \mid \bigcap_{h' < h} \mathcal{E}_{h'}^c] \Pr_{\pi^{\text{first}}}[\bigcap_{h' < h} \mathcal{E}_{h'}^c] \\ &= \Pr_{\pi^{\text{first}}}[\mathcal{E}_{s,h} \mid \bigcap_{h' < h} \mathcal{E}_{h'}^c] \Pr_{\pi^{\text{first}}}[\mathcal{E}_{h-1}^c \mid \bigcap_{h' < h-1} \mathcal{E}_{h'}^c] \Pr_{\pi^{\text{first}}}[\bigcap_{h' < h-1} \mathcal{E}_{h'}^c] \\ &\quad \vdots \\ &= \Pr_{\pi^{\text{first}}}[\mathcal{E}_{s,h} \mid \bigcap_{h' < h} \mathcal{E}_{h'}^c] \cdot \prod_{h' < h} \Pr_{\pi^{\text{first}}}[\mathcal{E}_{h'}^c \mid \bigcap_{h'' < h'} \mathcal{E}_{h''}^c]. \end{aligned}$$

If the event  $\bigcap_{h' < h} \mathcal{E}_{h'}^c$  holds, then up to step  $h$  no states are encountered for which  $T_{h'}(s) = 0$ . Thus, on such states,  $\pi^{\text{first}}$  and  $\pi^{\text{orc-first}}$  will behave identically. It follows that  $\mathbb{E}[\Pr_{\pi^{\text{first}}}[\mathcal{E}_{s,h} \mid \bigcap_{h' < h} \mathcal{E}_{h'}^c]] = \mathbb{E}[\Pr_{\pi^{\text{orc-first}}}[\mathcal{E}_{s,h} \mid \bigcap_{h' < h} \mathcal{E}_{h'}^c]]$ . By a similar argument, we have  $\Pr_{\pi^{\text{orc-first}}}[\mathcal{E}_{h'}^c \mid \bigcap_{h'' < h'} \mathcal{E}_{h''}^c] = \Pr_{\pi^{\text{first}}}[\mathcal{E}_{h'}^c \mid \bigcap_{h'' < h'} \mathcal{E}_{h''}^c]$  for each  $h' < h$ . Thus,

$$\Pr_{\pi^{\text{first}}}[\mathcal{E}_{s,h} \cap \bigcap_{h' < h} \mathcal{E}_{h'}^c] = \Pr_{\pi^{\text{orc-first}}}[\mathcal{E}_{s,h} \cap \bigcap_{h' < h} \mathcal{E}_{h'}^c].$$

It follows that

$$\mathbb{E}[\Pr_{\pi^{\text{first}}}[\mathcal{E}]] \leq \sum_{h \in [H]} \sum_{s \in \mathcal{S}} \mathbb{E}[\Pr_{\pi^{\text{orc-first}}}[\mathcal{E}_{s,h} \cap \bigcap_{h' < h} \mathcal{E}_{h'}^c]] \leq \sum_{h \in [H]} \sum_{s \in \mathcal{S}} \mathbb{E}[\Pr_{\pi^{\text{orc-first}}}[\mathcal{E}_{s,h}]].$$

From here the proof follows identically to the proof of Lemma A.8 of Rajaraman et al. (2020).  $\square$

*Proof of Theorem 1.* Set  $\lambda = \max\{A, 4 \log(HT)\}$  and  $\alpha = \frac{1}{\max\{A, H, \log(HT)\}}$ . We have

$$\mathcal{J}(\pi^\beta) - \mathbb{E}[\mathcal{J}(\hat{\pi}^{\text{bc}})] + \mathbb{E}[\mathcal{J}(\hat{\pi}^{\text{bc}})] - \mathbb{E}[\mathcal{J}(\tilde{\pi})] \lesssim \frac{H^2 S \log T}{T} + (1 + \alpha H) \cdot \frac{H^2 S \log T}{T} + \alpha \cdot \frac{H^2 S \lambda}{T}$$

where we bound  $\mathcal{J}(\pi^\beta) - \mathbb{E}[\mathcal{J}(\hat{\pi}^{\text{bc}})]$  by Theorem 4.4 of Rajaraman et al. (2020), and  $\mathbb{E}[\mathcal{J}(\hat{\pi}^{\text{bc}})] - \mathbb{E}[\mathcal{J}(\tilde{\pi})]$  by Lemma 2 since  $\lambda \geq 4 \log(HT)$ . By our choice of  $\alpha = \frac{1}{\max\{A, H, \log(HT)\}}$ , we can bound all of this as

$$\lesssim \frac{H^2 S \log T}{T}.$$

This proves the suboptimality guarantee. To show that  $\tilde{\pi}$  achieves demonstrator action coverage, we apply Lemma 1 using our values of  $\lambda$  and  $\alpha$ .  $\square$

#### B.4 Optimality of Posterior Demonstrator Policy

Let  $\mathcal{M}$  denote a multi-armed bandit with  $A > 1$  actions where  $r(a_1) = 1$  and  $r(a_i) = 0$  for  $i > 1$ . Let  $\pi^{\beta,i}$  denote the policy defined as

$$\pi^{\beta,i}(a) = \begin{cases} 1 - \alpha & a = 1 \\ \alpha & a = i \\ 0 & \text{o.w.} \end{cases}$$

for  $i > 1$  and  $\alpha$  some value we will set, and  $\pi^{\beta,1}(1) = 1$ . We let  $\mathcal{M}^i = (\mathcal{M}, \pi^{\beta,i})$  the instance-demonstrator pair,  $\mathbb{E}^i[\cdot]$  the expectation on this instance,  $\mathbb{P}^i$  the distribution on this instance, and  $\mathbb{P}^{i,T} = \otimes_{t=1}^T \mathbb{P}^i$ .

**Lemma 5.** *Consider the instance constructed above. Then we have that, for  $j \neq i$ :*

$$\mathbb{P}^i[\hat{\pi}(i) \geq \gamma \cdot \alpha] \leq 2 \cdot \mathbb{P}^j[\hat{\pi}(i) \geq \gamma \cdot \alpha] + T \cdot \alpha.$$

*Proof.* This follows from Lemma A.11 of Foster et al. (2021), which immediately gives that:

$$\mathbb{P}^i[\{\hat{\pi}(i) \geq \gamma \cdot \alpha\}] \leq 2 \cdot \mathbb{P}^j[\hat{\pi}(i) \geq \gamma \cdot \alpha] + D_H^2(\mathbb{P}^{i,T}, \mathbb{P}^{j,T}),$$

where  $D_H(\cdot, \cdot)$  denotes the Hellinger distance. Since the squared Hellinger distance is subadditive we have

$$D_H^2(\mathbb{P}^{i,T}, \mathbb{P}^{j,T}) \leq T \cdot D_H^2(\mathbb{P}^i, \mathbb{P}^j).$$

By elementary calculations we see that  $D_H^2(\mathbb{P}^i, \mathbb{P}^j) = \alpha$ , which proves the result.  $\square$

**Theorem 3** (Full version of Theorem 2). *Let  $\hat{\pi}$  achieve demonstrator action coverage with some parameter  $\gamma$  for each  $\mathcal{M}^i, i \in [A]$ , and some  $\delta \in (0, 1/4]$ , and assume that*

$$\mathcal{J}(\pi^{\beta,i}) - \mathbb{E}^i[\mathcal{J}(\hat{\pi})] \leq \xi, \quad \forall i \geq 1$$

for some  $\xi > 0$ . Then if  $T \leq \frac{1}{4\alpha}$ , it must be the case that

$$\gamma \leq \frac{\xi}{2A\alpha}.$$

In particular, setting  $\xi = c \cdot \frac{\log T}{T}$  and if  $\alpha = \frac{1}{2T}$ , we have

$$\gamma \leq c \cdot \frac{\log T}{A}.$$

*Proof.* Our goal is to find the maximum value of  $\gamma$  such that our constraint on the optimality of  $\hat{\pi}$  is met, for each  $\mathcal{M}^i$ . In particular, this can be upper bounded as

$$\max_{\hat{\pi}, \gamma} \gamma \quad \text{s.t.} \quad \mathbb{P}^i[\{\hat{\pi}(a) \geq \gamma \cdot \pi^{\beta}(a), \forall a \in \mathcal{A}\}] \geq 1 - \delta, \quad \mathcal{J}(\pi^{\beta,i}) - \mathbb{E}^i[\mathcal{J}(\hat{\pi})] \leq \xi, \quad \forall i \geq 1. \quad (5)$$

Note that for  $\mathcal{M}^i, i \geq 1$ , the event  $\{\hat{\pi}(a) \geq \gamma \cdot \pi^{\beta,i}(a), \forall a \in \mathcal{A}\}$  is a subset of the event  $\{\hat{\pi}(i) \geq \gamma \cdot \alpha\}$ . This allows us to bound (5) as

$$\max_{\hat{\pi}, \gamma} \gamma \quad \text{s.t.} \quad \mathbb{P}^i[\hat{\pi}(i) \geq \gamma \cdot \alpha] \geq 1 - \delta, \quad \mathcal{J}(\pi^{\beta,i}) - \mathbb{E}^i[\mathcal{J}(\hat{\pi})] \leq \xi, \quad \forall i \geq 1. \quad (6)$$

By Lemma 5, we have that for each  $i > 1$ ,

$$\mathbb{P}^i[\hat{\pi}(i) \geq \gamma \cdot \alpha] \leq 2 \cdot \mathbb{P}^1[\hat{\pi}(i) \geq \gamma \cdot \alpha] + T \cdot \alpha.$$

Furthermore, on  $\mathcal{M}^1$  we have  $\mathcal{J}(\pi^{\beta,1}) - \mathbb{E}^1[\mathcal{J}(\hat{\pi})] = \mathbb{E}^1[\sum_{i>1} \hat{\pi}(i)]$ . Given this, we can upper bound (6) as

$$\max_{\hat{\pi}, \gamma} \gamma \quad \text{s.t.} \quad \mathbb{P}^1[\hat{\pi}(i) \geq \gamma \cdot \alpha] \geq \frac{1}{2} \cdot (1 - \delta - T \cdot \alpha), \quad \forall i > 1, \quad \mathbb{E}^1[\sum_{i>1} \hat{\pi}(i)] \leq \xi. \quad (7)$$

By Markov's inequality, we have

$$\mathbb{P}^1[\hat{\pi}(i) \geq \gamma \cdot \alpha] \leq \frac{\mathbb{E}^1[\hat{\pi}(i)]}{\gamma \cdot \alpha}.$$

Furthermore, since we have assumed  $\delta \leq 1/4$  and  $T \leq \frac{1}{4\alpha}$ , we have  $\frac{1}{2} \cdot (1 - \delta - T \cdot \alpha) \geq \frac{1}{4}$ . We can therefore bound (7) as

$$\max_{\hat{\pi}, \gamma} \gamma \quad \text{s.t.} \quad \mathbb{E}^1[\hat{\pi}(i)] \geq \frac{1}{4} \cdot \gamma \alpha, \forall i > 1, \quad \mathbb{E}^1[\sum_{i>1} \hat{\pi}(i)] \leq \xi. \quad (8)$$

However, we see then that we immediately have

$$\gamma \leq \frac{\xi}{4(A-1)\alpha}.$$

This proves the result as long as  $A > 1$ .  $\square$

## C Posterior Demonstrator Policy for Gaussian Demonstrator

Let  $P(\cdot | \mu)$  denote the distribution  $\mathcal{N}(\mu, \Sigma)$ , where we assume  $\mu$  is unknown and  $\Sigma$  is known. Assume that we have samples  $\mathcal{D} = \{x_1, \dots, x_T\} \sim P(\cdot | \mu^*)$ . Let  $Q_{\text{prior}} = \mathcal{N}(0, \Lambda_0)$  denote the prior on  $\mu$ . Throughout this section we let  $=^d$  denote equality in distribution.

**Lemma 6.** *Under  $Q_{\text{prior}}$ , we have that the posterior  $Q_{\text{post}}$  on  $\mu$  is:*

$$Q_{\text{post}}(\cdot | \mathcal{D}) = \mathcal{N}\left(\Lambda_{\text{post}}\Sigma^{-1} \cdot \sum_{t=1}^T x_t, \Lambda_{\text{post}}\right),$$

for  $\Lambda_{\text{post}}^{-1} = \Lambda_0^{-1} + T \cdot \Sigma^{-1}$ .

*Proof.* Dropping terms that do not depend on  $\mu$ , we have

$$\begin{aligned} Q_{\text{post}}(\mu | \mathcal{D}) &= \frac{P(\mathcal{D} | \mu)Q_{\text{prior}}(\mu)}{P(\mathcal{D})} \\ &\propto \exp\left(-\frac{1}{2} \sum_{t=1}^T (x_t - \mu)^\top \Sigma^{-1} (x_t - \mu)\right) \cdot \exp\left(-\frac{1}{2} \mu^\top \Lambda_0 \mu\right) \\ &\propto \exp\left(-\frac{1}{2} T \mu^\top \Sigma^{-1} \mu - \frac{1}{2} \mu^\top Q_{\text{prior}}^{-1} \mu + \mu^\top \Sigma^{-1} \cdot \sum_{t=1}^T x_t\right) \\ &= \exp\left(-\frac{1}{2} (\mu - \Lambda_{\text{post}} v)^\top \Lambda_{\text{post}}^{-1} (\mu - \Lambda_{\text{post}} v) + \frac{1}{2} v^\top \Lambda_{\text{post}} v\right) \end{aligned}$$

for  $\Lambda_{\text{post}}^{-1} = \Lambda_0^{-1} + T \cdot \Sigma^{-1}$ , and  $v = \Sigma^{-1} \cdot \sum_{t=1}^T x_t$ .  $\square$

**Lemma 7** (General version of Proposition 4). *Let*

$$\hat{\mu} = \arg \min_{\mu} \sum_{t=1}^T (\mu - \tilde{x}_t)^\top \Sigma^{-1} (\mu - \tilde{x}_t) + (\mu - \tilde{\mu})^\top \Lambda_0^{-1} (\mu - \tilde{\mu}),$$

for  $\tilde{x}_t = x_t + w_t$ ,  $w_t \sim \mathcal{N}(0, \Sigma)$ , and  $\tilde{\mu} \sim Q_{\text{prior}}$ . Then  $\hat{\mu} =^d Q_{\text{post}}(\cdot | \mathcal{D})$ .

*Proof.* By computing the gradient of the objective, setting it equal to 0, and solving for  $\mu$ , we see that

$$\begin{aligned} \hat{\mu} &= (\Lambda_0^{-1} + T \Sigma^{-1})^{-1} \cdot \left( \Sigma^{-1} \cdot \sum_{t=1}^T \tilde{x}_t + \Lambda_0^{-1} \tilde{\mu} \right) \\ &= (\Lambda_0^{-1} + T \Sigma^{-1})^{-1} \cdot \Sigma^{-1} \cdot \sum_{t=1}^T x_t + (\Lambda_0^{-1} + T \Sigma^{-1})^{-1} \cdot \left( \Sigma^{-1} \cdot \sum_{t=1}^T w_t + \Lambda_0^{-1} \tilde{\mu} \right). \end{aligned}$$

Note that the first term in the above is deterministic conditioned on  $\mathcal{D}$ , and the second term is mean 0 and has covariance  $(\Lambda_0^{-1} + T \Sigma^{-1})^{-1}$ . We see then that the mean and covariance of  $\hat{\mu}$  match the mean the covariance of  $Q_{\text{post}}(\cdot | \mathcal{D})$  given in Lemma 6, which proves the result.  $\square$

## D Additional Experimental Details

For all experiments we instantiate POSTBC directly as suggested in Algorithm 1 and Algorithm 2. We describe additional details on this instantiation next.

In all experiments, we parameterize  $f_\ell$  in Algorithm 1 as an MLP (perhaps on top of a ResNet or other feature encoder, as described below). For the Robomimic experiments we let  $f_\ell$  parameterize a Gaussian distribution and seek to model the actions in the dataset with a Gaussian, for other settings we simply have  $f_\ell$  predict the actions directly (i.e. predicting a deterministic estimate of the actions rather than a distribution). Note that simply training  $f_\ell$  to predict the actions directly, rather than setting  $f_\ell$  to a generative model that seeks to model the entire action distribution, is consistent with Proposition 4—we aim to estimate a *sample* from the posterior distribution, for which it suffices to just fit a deterministic quantity, rather than fitting the entire *distribution* as generative modeling typically aims to do. Furthermore, fitting a simple predictor on the actions directly usually requires fewer training iterations than fitting, for example, a diffusion model to the entire distribution, so this also reduces the computation required to fit the ensemble.

We found in practice that using bootstrap sampling to generate the datasets  $\mathcal{D}_\ell$  in Algorithm 1 performs better than adding noise to the dataset as Proposition 4 suggests. We use both trajectory-level or state-action-level bootstrapping. For trajectory-level bootstrapping we generate  $\mathcal{D}_\ell$  as in Algorithm 3. For state-action-level bootstrapping we generate  $\mathcal{D}_\ell$  as in Algorithm 4. In all experiments

---

### Algorithm 3 Trajectory-Level Bootstrap Sampling

---

```

1: input: demonstration dataset  $\mathcal{D}$ 
2:  $\mathcal{D}_\ell \leftarrow \emptyset$ 
3: for  $t = 1, 2, \dots$ , number of trajectories in  $\mathcal{D}$  do
4:   Sample trajectory  $\tau \sim \text{unif}(\mathcal{D})$ 
5:    $\mathcal{D}_\ell \leftarrow \mathcal{D}_\ell \cup \{\tau\}$ 
6: return  $\mathcal{D}_\ell$ 

```

---



---

### Algorithm 4 Trajectory-Level Bootstrap Sampling

---

```

1: input: demonstration dataset  $\mathcal{D}$ 
2:  $\mathcal{D}_\ell \leftarrow \emptyset$ 
3: for  $t = 1, 2, \dots, |\mathcal{D}|$  do
4:   Sample state-action pair  $(s, a) \sim \text{unif}(\mathcal{D})$ 
5:    $\mathcal{D}_\ell \leftarrow \mathcal{D}_\ell \cup \{(s, a)\}$ 
6: return  $\mathcal{D}_\ell$ 

```

---

we parameterize our final policy with a diffusion model. Given this, Algorithm 2 is trained on the standard diffusion loss. Further details on each experiment are given below.

To leave room for RL improvement (i.e. to ensure performance is not saturated by the pretrained policy) we limit the number of demos per task in the pretraining dataset, for both the Robomimic and Libero experiments (see below for the precise number of trajectories used in pretraining).

### D.1 Robomimic Experiments

We instantiate  $\hat{\pi}^\theta$  with a diffusion policy that uses an MLP architecture. For  $f_\ell$ , we train an MLP to simply predict the action directly in  $\mathcal{D}_i$  (i.e. we do not use a diffusion model for  $f_\ell$ ), but use the same architecture and dimensions for  $f_\ell$  as the diffusion policies. We used trajectory-level bootstrapped sampling (Algorithm 3) to compute the ensemble. In all cases we pretrain on the Multi-Human Robomimic datasets, and in cases where we use less than the full dataset, we randomly select trajectories from the dataset to train on, using the same trajectories for each approach.

For each RL finetuning method, we sweep over the same hyperparameters for each pretrained policy method (i.e. BC,  $\sigma$ -BC, POSTBC), and include results for the best one. For  $\sigma$ -BC, we swept over values of  $\sigma$  and included results for the best-performing one. For all experiments results are averaged over 5 seeds (we pretrain 5 policies for each approach and run RL finetuning on each of them once,

for a total of 5 RL finetuning runs per pretraining method, finetuning method, and task). For each evaluation, we roll out the policy 200 times. For DPPO we utilize the default hyperparameters as stated in Ren et al. (2024), and utilize DDPM sampling. For VALUEDICE, we use the officially published codebase, and the default hyperparameters provided there. We found that the IQL training on the data produced by VALUEDICE could be somewhat unstable, and so to improve stability, for Lift, added LayerNorm to the IQL critic. For DSRL, we utilize a -1/0 success reward, and otherwise utilize a 0/1 success reward, using Robomimic’s built-in success detector to determine the reward. We provide hyperparameters for the individual experiments below.

Table 5: **Common DSRL hyperparameters for all experiments.**

Hyperparameter	Value
Learning rate	0.0003
Batch size	256
Activation	Tanh
Target entropy	0
Target update rate ( $\tau$ )	0.005
Number of actor and critic layers	3
Number of critics	2
Number of environments	4

Table 6: **DSRL hyperparameters for Robomimic experiments.**

Hyperparameter	Lift	Can	Square
Hidden size	2048	2048	2048
Gradient steps per update	20 (POSTBC, BC), 10 ( $\sigma$ -BC)	20 (POSTBC, BC), 10 ( $\sigma$ -BC)	20 (POSTBC, BC), 10 ( $\sigma$ -BC)
Noise critic update steps	20	10	10
Discount factor	0.99	0.99	0.999
Action magnitude	1.5	1.5	1.5
Initial steps	24000	24000	32000

Table 7: **Hyperparameters for pretrained policies for Robomimic DSRL experiments.**

Hyperparameter	Lift	Can	Square
Dataset size (number trajectories)	5	10	30
Action chunk size	4	4	4
train denoising steps	100	100	100
inference denoising steps	8	8	8
Hidden size	512	1024	1024
Hidden layers	3	3	3
Training epochs	3000	3000	3000
Ensemble size (POSTBC)	100	100	100
Ensemble training epochs (POSTBC)	10000	6000	3000
Posterior noise weight $\alpha$ (POSTBC)	1	0.5	1
Uniform noise $\sigma$ ( $\sigma$ -BC)	0.1	0.1	0.05

Table 8: **Best-of- $N$  hyperparameters for Robomimic experiments.**

Hyperparameter	Lift	Can	Square
Total gradient steps	2000000	2000000	2000000
IQL $\tau$ (1000 rollouts)	0.5 (BC, POSTBC), 0.7 ( $\sigma$ -BC), 0.9 (DICE)	0.7	0.7
IQL $\tau$ (2000 rollouts)	0.5 (BC), 0.7 ( $\sigma$ -BC, POSTBC), 0.9 (DICE)	0.7	0.7
Discount factor	0.999	0.999	0.999

Table 9: **Hyperparameters for pretrained policies for Robomimic Best-of- $N$  experiments.**

Hyperparameter	Lift	Can	Square
Dataset size (number trajectories)	20	300	300
Action chunk size	1	1	1
Train denoising steps	100	100	100
Hidden size	512	1024	1024
Hidden layers	3	3	3
Training epochs	3000	3000	3000
Ensemble size (POSTBC)	100 (1000 rollouts), 10 (2000 rollouts)	10	10
Ensemble training epochs (POSTBC)	3000	500	500
Posterior noise weight $\alpha$ (POSTBC)	1 (1000 rollouts), 2 (2000 rollouts)	1	1 (1000 rollouts), 2 (2000 rollouts)
Uniform noise $\sigma$ ( $\sigma$ -BC)	0.1	0.025	0.025

Table 10: **Hyperparameters for pretrained policies for Robomimic DPO experiments.**

Hyperparameter	Lift	Can	Square
Dataset size (number trajectories)	5	10	30
Action chunk size	4	4	4
train denoising steps	100	100	100
Hidden size	512	1024	1024
Hidden layers	3	3	3
Training epochs	3000	3000	3000
Ensemble size (POSTBC)	100	100	10
Ensemble training epochs (POSTBC)	3000	6000	3000
Posterior noise weight $\alpha$ (POSTBC)	0.5	0.25	1
Uniform noise $\sigma$ ( $\sigma$ -BC)	0.1	0.05	0.05

## D.2 Libero Experiments

For Libero, we utilize the transformer architecture from Dasari et al. (2024) for  $\hat{\pi}^\theta$ . For POSTBC we use state-action bootstrap sampling (Algorithm 3) to generate  $\mathfrak{D}_\ell$ . For  $f_\ell$ , we utilize the same ResNet and tokenizer as  $\hat{\pi}^\theta$ , but simply utilize a 3-layer MLP head on top of it—trained to predict the actions directly—rather than a full diffusion transformer. For the Best-of- $N$  experiments, POSTBC utilizes a diagonal posterior covariance estimate (that is, instead of computing the full covariance matrix as prescribed by Algorithm 1, we compute the covariance dimension-wise, and construct a diagonal covariance matrix from this), while for the DSRL runs it is trained with the full matrix posterior covariance estimate. We train on Libero 90 data from the first 3 scenes of Libero 90—KITCHEN SCENE 1, KITCHEN SCENE 2, and KITCHEN SCENE 3—and use 25 trajectories from each task in

each scene. For task conditioning, we conditioning  $\hat{\pi}^\theta$  on the BERT language embedding (Devlin et al., 2019) of the corresponding text given for that task in the Libero dataset.

For each RL finetuning method, we sweep over the same hyperparameters for each pretrained policy method (i.e. BC,  $\sigma$ -BC, POSTBC), and include results for the best one. We utilize the DSRL-SAC variant of DSRL from Wagenaaker et al. (2025a). For  $\sigma$ -BC, we swept over values of  $\sigma$  and included results for the best-performing one. The DSRL experiments are averaged over 3 different pretraining runs per method, and one DSRL run per pretrained run. The Best-of- $N$  experiments are averaged over 2 different pretraining runs per method. For each evaluation, we roll out the policy 100 times. In all cases, we utilize a -1/0 success reward, using Libero’s built-in success detector to determine the reward.

We provide hyperparameters for the individual experiments below.

Table 11: **DSRL hyperparameters for all Libero experiments.**

Hyperparameter	Value
Learning rate	0.0003
Batch size	256
Activation	Tanh
Target entropy	0
Target update rate ( $\tau$ )	0.005
Number of actor and critic layers	3
Layer size	1024
Number of critics	2
Number of environments	1
Gradient steps per update	20
Discount factor	0.99
Action magnitude	1.5
Initial episode rollouts	20

Table 12: **Best-of- $N$  hyperparameters for all Libero experiments.**

Hyperparameter	Value
IQL learning rate	0.0003
IQL batch size	256
IQL $\beta$	3
Activation	Tanh
Target update rate	0.005
$Q$ and $V$ number of layers	2
$Q$ and $V$ layer size	256
Number of critics	2
$N$ (Best-of- $N$ samples)	32
IQL gradient steps	50000
IQL $\tau$	0.9
Discount factor	0.99

Table 13: **Hyperparameters for DiT diffusion policy in Libero experiments.**

Hyperparameter	Value
Batch size	150
Learning rate	0.0003
Training steps	50000
LR scheduler	cosine
Warmup steps	2000
Action chunk size	4
Train denoising steps	100
Inference denoising steps	8
Image encoder	ResNet-18
Hidden size	256
Number of Heads	8
Number of Layers	4
Feedforward dimension	512
Token dimension	256
Ensemble size (POSTBC)	5
Ensemble training steps (POSTBC)	25000
Ensemble layer size	512
Ensemble number of layers	3
Posterior noise weight (POSTBC)	2 (DSRL run), 4 (Best-of- $N$ run)
Uniform noise $\sigma$ ( $\sigma$ -BC)	0.05

### D.3 WidowX Experiments



Figure 10: Setup for WidowX “Put corn in pot” task.



Figure 11: Setup for WidowX “Pick up banana” task.

For the WidowX experiment, we collect 10 demonstrations on the “Put corn in pot” task. For the diffusion policy, we utilize a U-Net architecture with ResNet image encoder. For the POSTBC ensemble predictors, we utilize a ResNet image encoder with MLP regression head, trained to directly predict the action in the dataset. For both BC and POSTBC, we pretrain the policy on the 10 demonstrations, then roll out the pretrained policy 100 times on each task, manually resetting the scene each time and classifying each trajectory as success or failure. We utilize a 0/1 reward (every step is given a reward of 0 unless it succeeds, when it is given a reward of 1). We then train an IQL  $Q$ -function on the rollout data and, at test time, roll out the pretrained policy, sampling  $N$  actions at each step, and choosing the action with the maximum  $Q$ -value. For IQL, we utilize an MLP-based architecture, and to process the images, we utilize image features from a ResNet encoder pretrained on the Bridge v2 dataset (Walke et al., 2023). For both BC and POSTBC, we try different values of  $N$  and different number of IQL training steps, and report the results for the best-performing values for each approach. All hyperparameters for the diffusion policy are given in Table 14, and for IQL in Table 15.

Table 14: **Hyperparameters for pretrained policies for WidowX experiments.**

Hyperparameter	Both WidowX tasks
Action chunk size	1
Train denoising steps	100
Inference denoising steps	16
Image encoder	ResNet-18
U-Net channel size	[256, 512, 1024]
U-Net kernel size	5
Training epochs	800
Ensemble predictor hidden size	512
Ensemble predictor hidden layers	3
Ensemble size (POSTBC)	10
Ensemble training epochs (POSTBC)	300
Posterior noise weight $\alpha$ (POSTBC)	1

Table 15: **Best-of- $N$  hyperparameters for WidowX experiments.**

Hyperparameter	Put corn in pot	Pick up banana
IQL learning rate	0.0003	0.0003
IQL batch size	256	256
IQL $\beta$	3	3
Activation	Tanh	Tanh
Target update rate	0.005	0.005
$Q$ and $V$ number of layers	2	2
$Q$ and $V$ layer size	256	256
Number of critics	2	2
$N$ (Best-of- $N$ samples)	4	16
IQL gradient steps	400000 (BC), 700000 (POSTBC)	100000
IQL $\tau$	0.7	0.7
Discount factor	0.97	0.97

#### D.4 Additional Ablations

For all ablation experiments, other than the hyperparameter we vary, we utilize the hyperparameters given in Section D.1. In Figure 12 we provide an additional ablation on the dataset size for `Robomimic Square`, and in Figure 13 provide additional qualitative results on `Libero`.

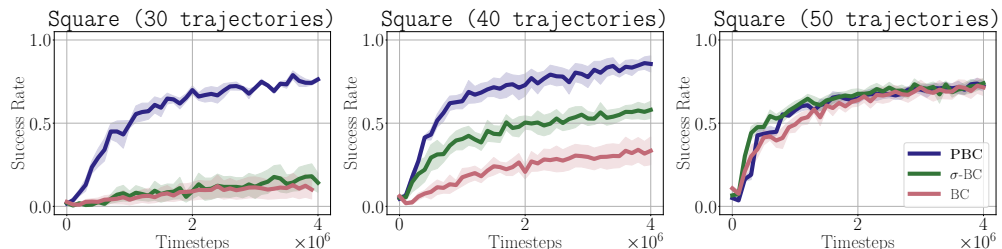


Figure 12: Comparison of DSRL finetuning performance combined with different BC pretraining approaches on `Robomimic Square`, varying the number of trajectories in the dataset the policies are pretrained on. As can be seen, the finetuning performance of policies pretrained with POSTBC is largely unaffected by the size of the pretraining dataset, while BC and  $\sigma$ -BC are both very sensitive to dataset size. For large enough datasets (50 trajectories), BC and  $\sigma$ -BC perform as well as POSTBC. This is to be expected—if we train on enough data, our uncertainty will be low, so POSTBC will essentially reduce to BC. These results illustrate that POSTBC gracefully interpolates between settings where BC overfits to small amounts of data, hurting its finetuning performance, and settings where BC is sufficient for effective finetuning.

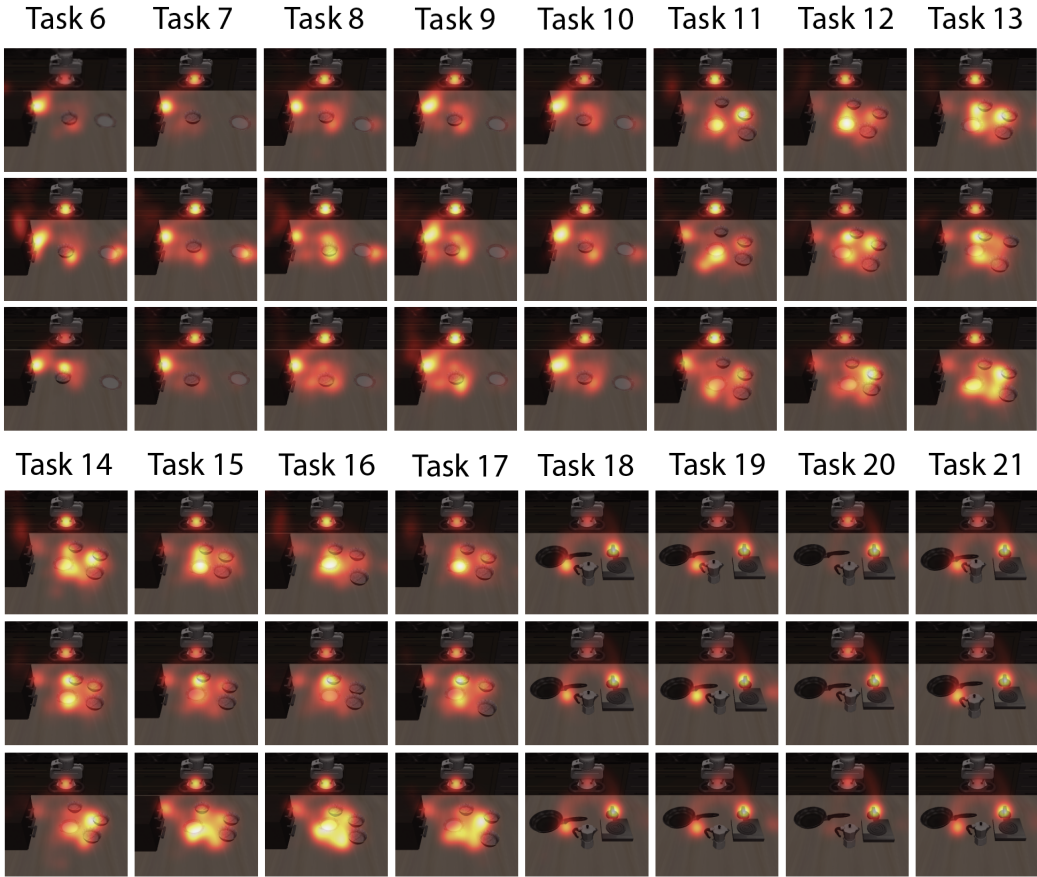


Figure 13: Additional density heatmaps of pretrained policies on tasks 6-21 from Libero 90. See Table 16 for task commands.

Table 16: **Task descriptions for Libero tasks in Kitchen Scene 1-3.**

Task ID	Task description
Task 6	Open the bottom drawer of the cabinet
Task 7	Open the top drawer of the cabinet
Task 8	Open the top drawer of the cabinet and put the bowl in it
Task 9	Put the black bowl on the plate
Task 10	Put the black bowl on top of the cabinet
Task 11	Open the top drawer of the cabinet
Task 12	Put the black bowl at the back on the plate
Task 13	Put the black bowl at the front on the plate
Task 14	Put the middle black bowl on the plate
Task 15	Put the middle black bowl on top of the cabinet
Task 16	Stack the black bowl at the front on the black bowl in the middle
Task 17	Stack the middle black bowl on the back black bowl
Task 18	Put the frying pan on the stove
Task 19	Put the moka pot on the stove
Task 20	Turn on the stove
Task 21	Turn on the stove and put the frying pan on it